



Validation of the Aura Microwave Limb Sounder ClO measurements

M. L. Santee,¹ A. Lambert,¹ W. G. Read,¹ N. J. Livesey,¹ G. L. Manney,^{1,2} R. E. Cofield,¹ D. T. Cuddy,¹ W. H. Daffer,¹ B. J. Drouin,¹ L. Froidevaux,¹ R. A. Fuller,¹ R. F. Jarnot,¹ B. W. Knosp,¹ V. S. Perun,¹ W. V. Snyder,¹ P. C. Stek,¹ R. P. Thurstans,¹ P. A. Wagner,¹ J. W. Waters,¹ B. Connor,³ J. Urban,⁴ D. Murtagh,⁴ P. Ricaud,⁵ B. Barret,⁵ A. Kleinböhl,¹ J. Kuttippurath,^{6,7} H. Küllmann,⁶ M. von Hobe,⁸ G. C. Toon,¹ and R. A. Stachnik¹

Received 6 April 2007; revised 31 October 2007; accepted 16 December 2007; published 14 May 2008.

[1] We assess the quality of the version 2.2 (v2.2) ClO measurements from the Microwave Limb Sounder (MLS) on the Earth Observing System Aura satellite. The MLS v2.2 ClO data are scientifically useful over the range 100 to 1 hPa, with a single-profile precision of ~ 0.1 ppbv throughout most of the vertical domain. Vertical resolution is ~ 3 –4 km. Comparisons with climatology and correlative measurements from a variety of different platforms indicate that both the amplitude and the altitude of the peak in the ClO profile in the upper stratosphere are well determined by MLS. The latitudinal and seasonal variations in the ClO distribution in the lower stratosphere are also well determined, but a substantial negative bias is present in both daytime and nighttime mixing ratios at retrieval levels below (i.e., pressures larger than) 22 hPa. Outside of the winter polar vortices, this negative bias can be eliminated by subtracting gridded or zonal mean nighttime values from the individual daytime measurements. In studies for which knowledge of lower stratospheric ClO mixing ratios inside the winter polar vortices to better than a few tenths of a ppbv is needed, however, day – night differences are not recommended and the negative bias must be corrected for by subtracting the estimated value of the bias from the individual measurements at each affected retrieval level.

Citation: Santee, M. L., et al. (2008), Validation of the Aura Microwave Limb Sounder ClO measurements, *J. Geophys. Res.*, 113, D15S22, doi:10.1029/2007JD008762.

1. Introduction

[2] The partitioning between active and reservoir forms of chlorine modulates ozone destruction throughout the stratosphere [e.g., Solomon, 1999; World Meteorological Organization, 2007]. Chlorine monoxide, ClO, is the primary form of reactive chlorine in the stratosphere and thus a key catalyst for ozone loss. The Microwave Limb Sounder (MLS) on NASA's Earth Observing System (EOS) Aura satellite measures vertical profiles of ClO globally on a daily basis. Initial validation of the first publicly available Aura MLS ClO data

set, version 1.5 (v1.5), was presented by Barret *et al.* [2006]. Here we report on the quality of the recently released version 2.2 (v2.2) Aura MLS ClO measurements. The measurement system is described in section 2. In addition to providing a review of instrumental and orbital characteristics, this section includes guidelines for quality control that should be applied to the v2.2 ClO measurements, documents their precision and spatial resolution, and quantifies sources of systematic uncertainty. Because the v1.5 Aura MLS ClO data have been featured in some previous studies [e.g., Schoeberl *et al.*, 2006a; Santee *et al.*, 2005], section 2 provides an overview of the differences between v2.2 and v1.5 ClO data. A systematic negative bias, present in v1.5 but, unfortunately, worse in v2.2, is also quantified in this section. In section 3, “zeroth-order” validation of the Aura MLS ClO data is accomplished by comparing against climatological averages in narrow equivalent latitude bands compiled from the multiyear Upper Atmosphere Research Satellite (UARS) MLS ClO data set. Accuracy is assessed through comparisons with correlative data sets from a variety of platforms in section 4. Finally, in section 5 we summarize the Aura MLS ClO validation results.

2. Aura MLS ClO Measurement Description

2.1. Overview of the MLS Measurement System

[3] Aura, the last in NASA's EOS series of satellites, was launched on 15 July 2004 into a near-polar, sun-synchronous,

¹Jet Propulsion Laboratory, California Institute of Technology, Pasadena, California, USA.

²Also at Department of Physics, New Mexico Institute of Mining and Technology, Socorro, New Mexico, USA.

³National Institute of Water and Atmospheric Research, Omakau, New Zealand.

⁴Department of Radio and Space Science, Chalmers University of Technology, Göteborg, Sweden.

⁵Laboratoire d'Aérodynamique, Observatoire de Midi-Pyrénées, Toulouse, France.

⁶Institute of Environmental Physics, University of Bremen, Bremen, Germany.

⁷Now at LMD/CNRS Ecole Polytechnique, Palaiseau, France.

⁸Institut für Chemie und Dynamik der Geosphäre I: Stratosphäre, Forschungszentrum Jülich, Jülich, Germany.

705-km altitude orbit with a 1345 local time (LT) ascending equator-crossing time [Schoeberl *et al.*, 2006b]. One of its four instruments, Aura MLS, is an advanced successor to the Microwave Limb Sounder on UARS. Detailed information on the microwave limb sounding technique in general and the Aura MLS instrument in particular is given by Waters [1993] and Waters *et al.* [2006], respectively. MLS observes a large suite of atmospheric parameters by measuring millimeter- and submillimeter-wavelength thermal emission from Earth's limb with seven radiometers covering five broad spectral regions. The standard CIO product is retrieved from radiances measured by the radiometer centered near 640 GHz, which covers the strong CIO rotational line at 649.5 GHz. CIO is also measured by the 190-GHz radiometer (using the 204.4 GHz CIO line measured by UARS MLS), but these retrievals have slightly poorer precision and are not considered further here.

[4] The Aura MLS fields of view point forward in the direction of orbital motion and vertically scan the limb in the orbit plane, leading to data coverage from 82°S to 82°N latitude on every orbit. Thus Aura MLS obtains continuous daily sampling of both polar regions, with none of the temporal gaps from yaw maneuvers that occurred with UARS MLS. The MLS limb scans are synchronized to the Aura orbit, with 240 scans per orbit at essentially fixed latitudes. This results in ~3500 scans per day, with an along-track separation between adjacent retrieved profiles of 1.5° great circle angle (~165 km). The longitudinal separation of MLS measurements, set by the Aura orbit, is 10–20° over low and middle latitudes, with much finer sampling in the polar regions. Most MLS data products, including CIO, are reported on a fixed vertical pressure grid with six levels per decade change in pressure in the troposphere and stratosphere.

[5] The MLS “Level 2” data (retrieved geophysical parameters and diagnostics at the measurement locations along the suborbital track) are generated from input “Level 1” data (calibrated radiances and engineering information) by the MLS data processing software. The MLS retrieval algorithms, described in detail by Livesey *et al.* [2006], are based on the standard optimal estimation method; they employ a two-dimensional approach that takes into account the fact that limb observations from consecutive scans cover significantly overlapping regions of the atmosphere. The data are divided into overlapping “chunks” consisting of the measurements in a 15° span of great circle angle (typically about 10 vertical profiles); retrievals are performed for each of these chunks independently and then joined together to produce a complete set of output [Livesey *et al.*, 2006]. The results are reported in Level 2 Geophysical Product (L2GP) files, which are HDF-EOS (a version of the Hierarchical Data Format developed specifically for storing Earth science data generated by EOS instruments) version 5 files containing swaths in the Aura-wide standard format [Livesey *et al.*, 2007]. A separate L2GP file is produced for each standard MLS product for each day (0000–2400 UT).

[6] Reprocessing of the MLS data collected to date with the v2.2 algorithms is ongoing; however, at the time of writing (February 2007) only a small subset of the data, consisting of fewer than 100 days, has been reprocessed, with priority given to days for which correlative measure-

ments exist. Although small compared to the entire MLS data record, this set of v2.2 days spans all seasons and is sufficient for thorough investigation of the MLS data quality.

2.2. MLS CIO Data Usage Guidelines

[7] Along with the data fields, the L2GP files contain corresponding precision fields, which quantify the impact of radiance noise on the data and, particularly in regions with less measurement sensitivity, the contribution of a priori information. The data processing software flags the precision with a negative sign when the estimated precision is worse than 50% of the a priori precision; thus only data points for which the associated precision value is positive should be used.

[8] Three additional data quality metrics are provided for every vertical profile of each product. “Status” is a bit field indicating operational abnormalities or problems with the retrievals; see Table 1 for a complete description. Profiles for which “Status” is an odd number should not be used in any scientific study. Nonzero but even values of “Status” indicate that the profile has been marked as questionable, typically because the measurements may have been affected by the presence of thick clouds. Globally fewer than 1% of profiles are typically identified in this manner, and clouds generally have little influence on the stratospheric CIO data. Thus profiles with even values of “Status” may be used without restriction.

[9] The “Quality” field describes the degree to which the measured MLS radiances have been fitted by the Level 2 algorithms. In theory, larger values of “Quality” indicate generally good radiance fits, whereas values closer to zero indicate poorer radiance fits and thus less reliable data. In practice, low values of “Quality” are not always associated with profiles that are obviously “bad.” As a precaution, we recommend rejecting profiles having “Quality” values less than 0.8. This threshold for “Quality” typically excludes ~1–3% of CIO profiles on a daily basis; it is a conservative value that potentially discards a significant fraction of “good” data points while not necessarily identifying all “bad” ones.

[10] Additional information on the success of the retrieval is conveyed by the “Convergence” field, which compares the fit achieved for each “chunk” of ~10 profiles to that expected by the retrieval algorithms; values around 1.0 typically indicate good convergence. We recommend rejecting profiles for which “Convergence” exceeds 1.5. On a typical day this threshold for “Convergence” discards 2–5% of the CIO profiles, some (but not all) of which are filtered out by the other quality control measures.

[11] Finally, we note that the MLS data processing algorithms often produce negative mixing ratios, especially for noisy retrievals such as CIO when values are very low. Though unphysical, the negative mixing ratios must be retained in any scientific studies making use of averages of data, in order to avoid introducing positive biases into the MLS averages.

2.3. Signature of CIO in the MLS Radiances

[12] Sample radiances from the 640-GHz region of the spectrum for a representative day during Antarctic winter are shown in Figure 1. More specifics about the MLS

Table 1. Meaning of Bits in the “Status” Field

Bit	Value ^a	Meaning
0	1	flag: do not use this profile (see bits 8–9 for details)
1	2	flag: this profile is “suspect” (see bits 4–6 for details)
2	4	unused
3	8	unused
4	16	information: this profile may have been affected by high-altitude clouds
5	32	information: this profile may have been affected by low-altitude clouds
6	64	information: this profile did not use GEOS-5 temperature a priori data
7	128	unused
8	256	information: retrieval diverged or too few radiances available for retrieval
9	512	information: the task retrieving data for this profile crashed (typically a computer failure)

^a“Status” field in L2GP file is the total of appropriate entries in this column.

spectrometers, the spectral bands they cover, and their target molecules are given by *Waters et al.* [2006], and a full representation of the MLS spectral coverage superimposed on a calculated atmospheric spectrum is presented by *Read et al.* [2006]. The dominant spectral feature in Figure 1 (top) is due to emission from an O₃ line near 650.7 GHz in the upper sideband (upper x axis); the smaller peak at

649.45 GHz arises from a cluster of ClO lines. Figure 1 (left) shows global average radiances, while Figure 1 (right) shows the region poleward of 60°S (where chlorine has been converted from reservoir forms to ClO inside the Antarctic polar vortex) in order to emphasize the ClO spectral signature, which typically has an amplitude of ~10–15 K in the lower stratosphere when ClO is enhanced. The residuals shown in Figure 1 (bottom) indicate that on average the retrievals are fitting the radiances to within ~5% (~0.5 K) for these bands.

2.4. Precision, Spatial Resolution, and Vertical Range

[13] The precision of the MLS ClO measurements is estimated empirically by computing the standard deviation of the descending (i.e., nighttime) profiles in the 20°-wide latitude band centered around the equator. For this region and time of day, natural atmospheric variability should be negligible relative to the measurement noise. As shown in Figure 2, the observed scatter in the v2.2 data is ~0.1 ppbv from 100 to 3 hPa, rising to ~0.3 ppbv at 1 hPa, above which it increases sharply. The scatter is essentially invariant with time, as seen by comparing the results for the different days shown in Figure 2.

[14] The single-profile precision estimates cited here are, to first order, independent of latitude and season, but it should be borne in mind that the scientific utility of individual MLS profiles (i.e., signal to noise) varies with ClO abundance. Outside of the lower stratospheric winter polar vortices, within which ClO is often strongly enhanced,

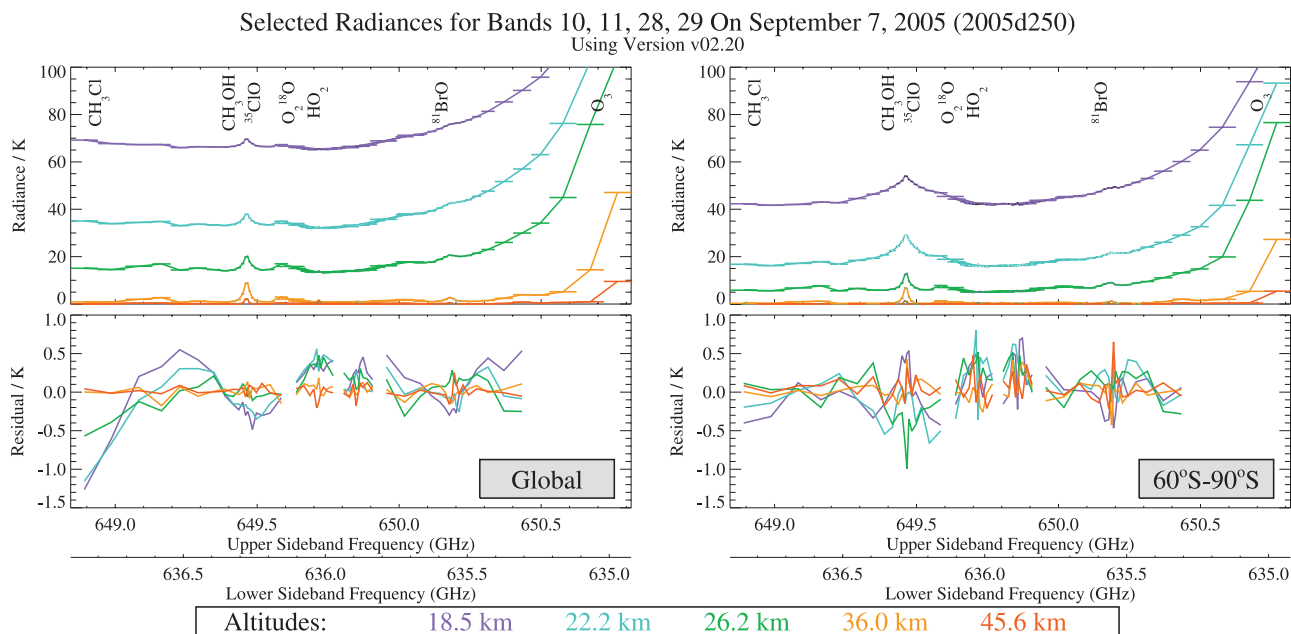


Figure 1. Sample radiances and residuals from the Aura MLS 640-GHz radiometer for bands 10 and 11 for ascending (daytime) data averaged over (left) the entire globe and (right) latitudes poleward of 60°S. (top) Average radiances for a representative day with substantial ClO enhancement in the Antarctic polar vortex (7 September 2005), expressed as brightness temperature (in K), for five selected tangent point altitudes from 18.5 km (purple) to 45.6 km (red). The MLS signal is a combination of incoming radiance at frequencies above (upper sideband, upper x axis) and below (lower sideband, lower x axis) the 642.870 GHz local oscillator. The widths of the various MLS spectral channels are denoted by the horizontal bars. (bottom) The average residual of the fit achieved by the MLS version 2.2 (v2.2) retrieval algorithms. Residuals for channels not used in the retrievals are not shown.

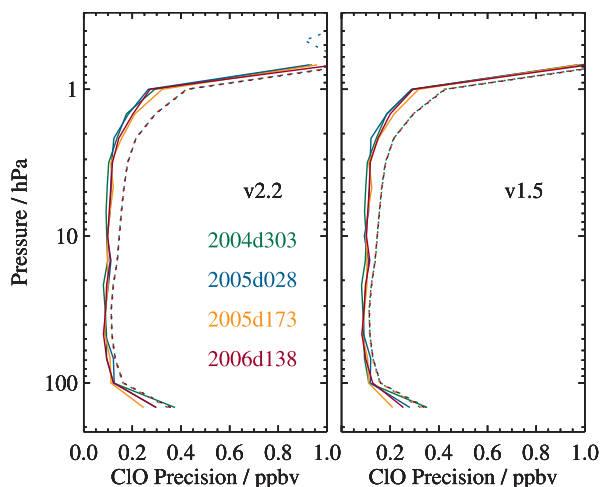


Figure 2. Precision of the (left) v2.2 and (right) v1.5 MLS CIO measurements for four representative days (see legend). Solid lines depict the observed scatter in nighttime-only measurements obtained in a narrow equatorial band (see text); dotted lines depict the theoretical precision estimated by the retrieval algorithm.

the single-profile precision exceeds typical CIO mixing ratios, necessitating the use of averages for scientific studies. In most cases, precision can be improved by averaging, with the precision of an average of N profiles being $1/\sqrt{N}$ times the precision of an individual profile (note that this is not the case for averages of successive along-track profiles, which are not completely independent because of horizontal smearing).

[15] The observational determination of the precision is compared in Figure 2 to the theoretical precision values reported by the Level 2 data processing algorithms. The predicted precision exceeds the observed scatter, particularly above 15 hPa. This is a common feature of optimal estimation retrieval systems, indicating that the a priori information and the vertical smoothing applied to stabilize the retrieval are having a nonnegligible influence by reducing the variability in the retrieved values at these levels. Because the theoretical precisions take into account occasional variations in instrument performance, the best estimate of the precision of an individual data point is the value quoted for that point in the L2GP files, but it should be borne in mind that this approach can slightly overestimate the actual measurement noise.

[16] For comparison, Figure 2 also shows precision estimates for the v1.5 MLS CIO data. In terms of precision, the v2.2 CIO data are not greatly different from v1.5; other differences between the two versions are discussed in section 2.6.

[17] As mentioned previously, the MLS retrieval algorithms employ a two-dimensional approach that accounts for the fact that the radiances for each limb scan are influenced by the state of the atmosphere at adjacent scans along the forward looking instrument line of sight [Livesey *et al.*, 2006]. The resolution of the retrieved data can be described using “averaging kernels” [e.g., Rodgers, 2000]; the two-dimensional nature of the MLS data processing system means that the kernels describe both vertical and

horizontal resolution. Smoothing, imposed on the retrieval system in both the vertical and horizontal directions to enhance retrieval stability and precision, degrades the inherent resolution of the measurements. Consequently, the vertical resolution of the v2.2 CIO data, as determined from the full width at half maximum of the rows of the averaging kernel matrix shown in Figure 3, is ~ 3 – 4.5 km. Note that there is considerable overlap in the averaging kernels for the 100 and 147 hPa retrieval surfaces, indicating that the 147 hPa retrieval does not provide completely independent information. Figure 3 also shows horizontal averaging kernels, from which the along-track horizontal resolution is determined to be ~ 250 – 500 km over most of the vertical range. The cross-track resolution, set by the width of the field of view of the 640-GHz radiometer, is ~ 3 km.

[18] Although CIO is retrieved (and reported in the L2GP files) over the range from 147 to 0.001 hPa, on the basis of the drop off in precision and resolution and the lack of independent information contributed by the measurements, the data are not deemed reliable at the extremes of the retrieval range. Thus we recommend that v2.2 CIO be used for scientific studies only at the levels between 100 and 1 hPa.

2.5. Quantification of Systematic Uncertainty

[19] A major component of the validation of MLS data is the quantification of the various sources of systematic uncertainty. Systematic uncertainties arise from instrumental issues (e.g., radiometric calibration, field of view characterization), spectroscopic uncertainty, and approximations in the retrieval formulation and implementation. This section summarizes the relevant results of a comprehensive quantification of these uncertainties that was performed for all MLS products. More information on this assessment is given by Read *et al.* [2007, Appendix A].

[20] The impact on MLS measurements of radiance (or pointing where appropriate) of each identified source of systematic uncertainty has been quantified and modeled. These modeled impacts correspond to either $2\text{-}\sigma$ estimates of uncertainties in the relevant parameters, or an estimate of their maximum reasonable errors based on instrument knowledge and/or design requirements. The effect of these perturbations on retrieved MLS products has been quantified for each source of uncertainty by one of two methods.

[21] In the first method, sets of modeled errors corresponding to the possible magnitude of each uncertainty have been applied to simulated MLS cloud-free radiances, based on a model atmosphere, for a whole day of MLS observations. These sets of perturbed radiances have then been run through the routine MLS data processing algorithms, and the differences between these runs and the results of the “unperturbed” run have been used to quantify the systematic uncertainty in each case. The impact of the perturbations varies from product to product and among uncertainty sources. Although the term “systematic uncertainty” is often associated with consistent additive and/or multiplicative biases, many sources of “systematic” uncertainty in the MLS measurement system give rise to additional scatter in the products. For example, although an error in the O_3 spectroscopy is a bias on the fundamental parameter, it has an effect on the retrievals of species with weaker signals (e.g., CIO) that is dependent on the amount and morphology of atmospheric ozone. The extent to which

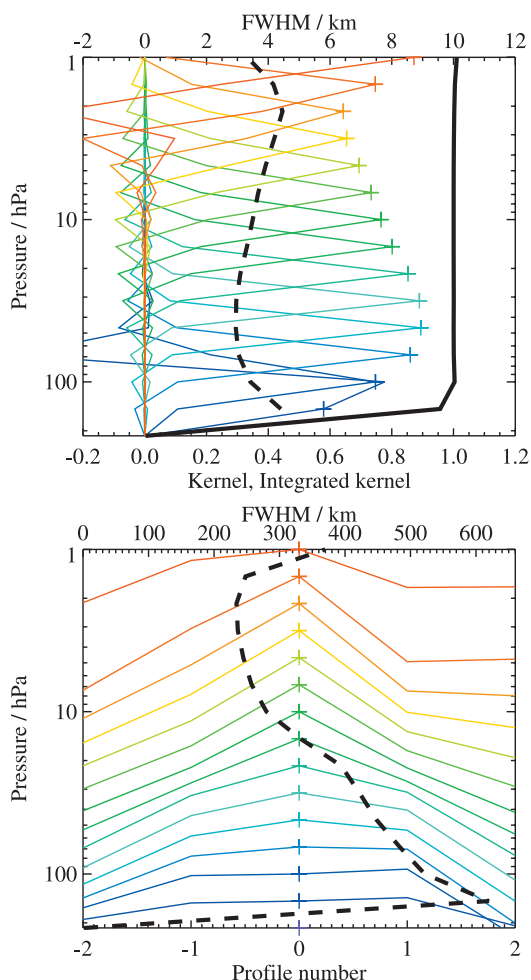


Figure 3. Typical two-dimensional (vertical and horizontal along-track) averaging kernels for the MLS v2.2 ClO data at 70°N; variation in the averaging kernels is sufficiently small that these are representative for all profiles. Colored lines show the averaging kernels as a function of MLS retrieval level, indicating the region of the atmosphere from which information is contributing to the measurements on the individual retrieval surfaces, which are denoted by plus signs in corresponding colors. The dashed black line indicates the resolution, determined from the full width at half maximum (FWHM) of the averaging kernels, approximately scaled into kilometers (top axis). (top) Vertical averaging kernels (integrated in the horizontal dimension for five along-track profiles) and resolution. The solid black line shows the integrated area under each kernel (horizontally and vertically); values near unity imply that the majority of information for that MLS data point has come from the measurements, whereas lower values imply substantial contributions from a priori information. (bottom) Horizontal averaging kernels (integrated in the vertical dimension) and resolution. The individual horizontal averaging kernels are scaled in the vertical direction such that a unit change is equivalent to one decade in pressure.

such terms can be expected to average down is estimated to first order by these “full up studies” through their separate consideration of the bias and scatter each source of uncertainty introduces into the data. The difference between the retrieved product in the unperturbed run and the original “truth” model atmosphere is taken as a measure of uncertainties due to retrieval formulation and numerics. To test the sensitivity of the retrieved mixing ratios to the a priori information, another retrieval of the unperturbed radiances is performed with the a priori adjusted by a factor of 1.5.

[22] In the second method, the potential impact of some remaining (typically small) systematic uncertainties has been quantified through calculations based on simplified models of the MLS measurement system [see *Read et al., 2007*]. Unlike the “full up studies,” these calculations only provide estimates of “gain uncertainty” (i.e., possible multiplicative error) introduced by the source in question; this approach does not quantify possible biases or additional scatter for these minor sources of uncertainty.

[23] Figure 4 summarizes the results of the error characterization for the MLS v2.2 ClO measurements. The colored lines show the magnitudes of expected biases, additional scatter, and possible scaling uncertainties the various errors may introduce into the data, and should be interpreted as $2\text{-}\sigma$ estimates of their probable magnitude. The dominant source of uncertainty throughout the profile originates from the spectral distortion induced in the calibrated MLS radiances by departures from a linear response within the signal chains, leading to gain compression. The exact nature of this distortion has yet to be fully characterized; however, a representative signature has been used to estimate the resultant uncertainty (cyan lines). Other potentially significant sources of error include uncertainty in the field of view pointing offsets between the two 118-GHz radiometers and the 240-GHz radiometer (red lines), uncertainty in continuum emission/absorption and the width of the spectral line measured by MLS (green lines), and the impact of errors in O_3 (retrieved in the same phase as ClO [*Livesey et al., 2006*]) arising from errors in the O_3 line shape (blue lines). Retrieval numerics and sensitivity of the MLS measurement system to a priori information (grey lines) contribute some scatter throughout the vertical range. Although these simulation results also suggest that retrieval numerics may lead to scaling errors of $\pm 35\text{--}55\%$ at 68 and 100 hPa, a reliable estimate is hampered by the (albeit geophysically appropriate) lack of dynamic range in the “truth” mixing ratios used for these levels, and the actual multiplicative error contributed by retrieval numerics is likely to be much smaller (e.g., $\sim \pm 20\%$ as at 46 hPa). Other potential sources of uncertainty, such as the presence of thick clouds associated with deep convection or errors in the MLS temperature product, are found to have a negligible impact.

[24] In aggregate, systematic uncertainties are estimated to induce in the v2.2 ClO measurements biases of $\sim \pm 0.1$ ppbv from 100 to 32 hPa and less than ± 0.05 ppbv above 22 hPa and multiplicative errors of $\sim \pm 5\text{--}20\%$ throughout the stratosphere. The scatter introduced into the data by the various sources of uncertainty is estimated to be less than ± 0.04 ppbv throughout the vertical domain, a value substantially smaller than the empirical determination of the precision ($\sim 0.1\text{--}0.3$ ppbv) discussed in section 2.4.

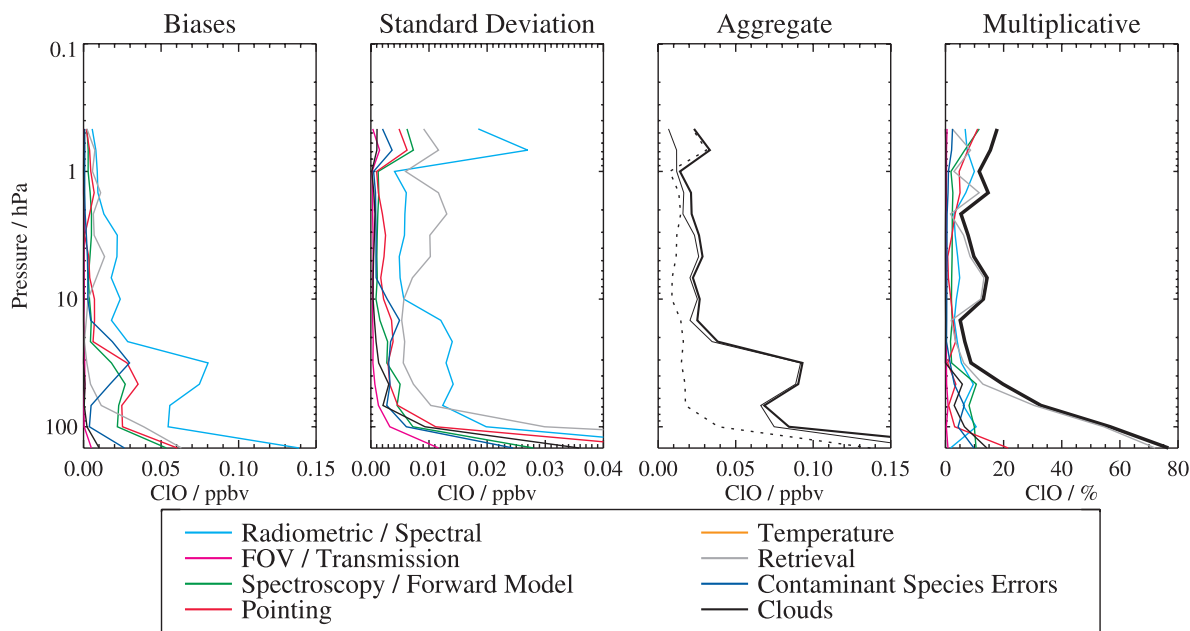


Figure 4. The estimated impact ($2\text{-}\sigma$) of various families of systematic uncertainty on the MLS CIO observations. The first two panels show the possible biases (first panel) and standard deviation (second panel) of the additional scatter introduced by the various families of uncertainty, with each family denoted by a different colored line. Cyan lines denote uncertainties in MLS radiometric and spectral calibration. Magenta lines show uncertainties associated with the MLS field of view and antenna transmission efficiency. Red lines depict errors associated with MLS pointing uncertainty. The impacts of uncertainties in spectroscopic databases and forward model approximations are denoted by the green line, while those associated with retrieval formulation are shown in grey. The gold lines indicate uncertainty resulting from errors in the MLS temperature product, while the blue lines show the impact of similar “knock on” errors in other species. Finally, the typical impact of cloud contamination is denoted by the black line. The third panel shows the root sum square (RSS) of all the possible biases (thin solid line), all the additional scatter (thin dotted line), and the RSS sum of the two (thick solid line). The fourth panel shows the scaling uncertainty introduced by the various families of errors, with the thick black line showing the RSS of all the reported scaling uncertainties.

[25] As will be discussed in more detail in the following sections, a substantial ($\sim 0.1\text{--}0.4$ ppbv) negative bias is present in the v2.2 MLS CIO measurements at retrieval levels below 22 hPa. That such a significant feature in the data is not explained by the results presented in Figure 4 indicates limitations in our uncertainty quantification study. Potential but unaccounted for sources of error include contamination of the CIO retrieval from interfering species (other than ozone, the impact of which was quantified in Figure 4). Possible contaminant species include CH_3Cl , which has lines in two wing channels of the band used to measure CIO, and CH_3OH , which has a cluster of lines in the image sideband with an intermediate frequency nearly the same as that of CIO. Experiments with precursory “version 3” algorithms in which CH_3Cl is retrieved show great promise in reducing the negative bias in the lower stratospheric CIO data, as shown in Figure 5. Although rigorous validation of the resulting CH_3Cl field has not yet been undertaken, preliminary investigations suggest that the morphology of the retrieved CH_3Cl profiles is physically reasonable compared to previous measurements [e.g., Toon *et al.*, 1999; Nassar *et al.*, 2006]. Adding CH_3OH to the retrieval yields only a modest further improvement in the CIO bias (Figure 5). Although more development and

testing are needed, our initial results indicate that inclusion of these additional species in the MLS retrieval system reduces the negative bias in CIO to values in line with the systematic error analysis.

2.6. Comparison With v1.5 CIO Data

[26] Early validation analyses of the v1.5 Aura MLS CIO data [Livesey *et al.*, 2005] revealed a persistent negative bias of as much as ~ 0.3 ppbv at low and middle latitudes in both daytime and nighttime mixing ratios at the lowest retrieval levels (below about 32 hPa). Comparisons with coincident measurements of CIO from the Submillimetre Radiometer (SMR) on board the Odin satellite confirmed a systematic low bias of this magnitude in the MLS v1.5 data outside of the winter polar regions [Barret *et al.*, 2006].

[27] Figure 6, which shows the comparison between v1.5 and v2.2 for 93 days for which both versions of data were available at the time of writing (February 2007), indicates that the negative bias has been exacerbated in v2.2, with the mixing ratios at 100 hPa more than 0.1 ppbv lower than they were in v1.5 in the global average. Small differences between v1.5 and v2.2 are evident elsewhere in the profile as well; maximum mixing ratios at the profile peak in the lower stratosphere are slightly larger, whereas mixing ratios

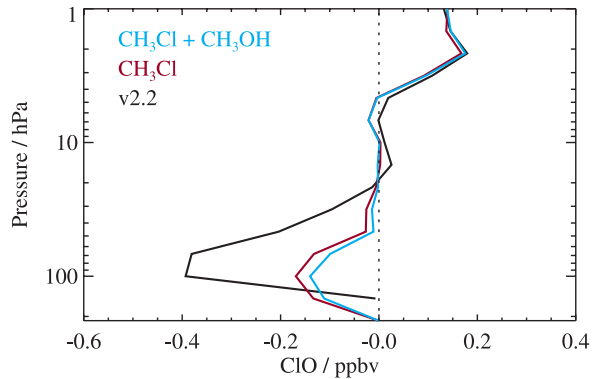


Figure 5. Comparison of mean nighttime (descending) CIO profiles averaged over the region 25°S – 25°N from v2.2 processing (black) and from precursory “version 3” algorithms in which CH_3Cl (red) and CH_3OH (cyan) are also retrieved.

at the secondary peak near 2–3 hPa are slightly smaller (both by ~ 0.02 ppbv in the global mean) than they were in v1.5. The differences in peak values in both the upper and lower stratosphere can also be seen in the zonal mean fields in Figure 7.

[28] Differences between the v1.5 and v2.2 retrieval algorithms giving rise to these effects include changes in the representation of the continuum emission for the 640-GHz region, incorporation of additional O_3 lines, use of new direct laboratory measurements of O_3 line widths (including for isotopic and vibrational state lines) for several lines in this region, use of an updated version of the HITRAN database (2004 rather than 2000), and changes

in the tangent pressure retrieval. These refinements led to substantial improvements in most MLS data products. Although cumulatively they resulted in an increase in the severity of the negative bias in CIO at the lowest retrieval levels, nevertheless the v2.2 CIO retrieval is considered more reliable as other compensating errors have been eliminated. We therefore strongly recommend the use of v2.2, rather than v1.5, MLS CIO measurements for scientific studies.

2.7. Quantification of the Systematic Negative Bias

[29] To quantify the magnitude of the negative bias in the v2.2 MLS CIO data and look for possible latitudinal and temporal variations in it, we have examined time series of data from the ascending (primarily daytime) and descending (primarily nighttime) sides of the orbit, as well as ascending – descending (day – night) difference values for all days that have so far been reprocessed in v2.2 (93 days spanning the time since launch in July 2004 through February 2007). The data have been binned and averaged in 10° -wide equivalent latitude bands between 80°S and 80°N on the 660, 580, 520, 460, and 410 K potential temperature surfaces, corresponding to pressure levels of 22, 32, 46, 68, and 100 hPa, respectively; as an example, Figure 8 shows the results for 460 K. Averages were calculated in equivalent latitude (EqL, the latitude encircling the same area as a given contour of potential vorticity (PV) [Butchart and Remsberg, 1986]) rather than geographic latitude to obtain a vortex-centered view, ensuring that only similar air masses are averaged together and segregating the regions of CIO enhancement inside the winter polar vortex from the extravortex regions, where CIO mixing ratios are generally very low.

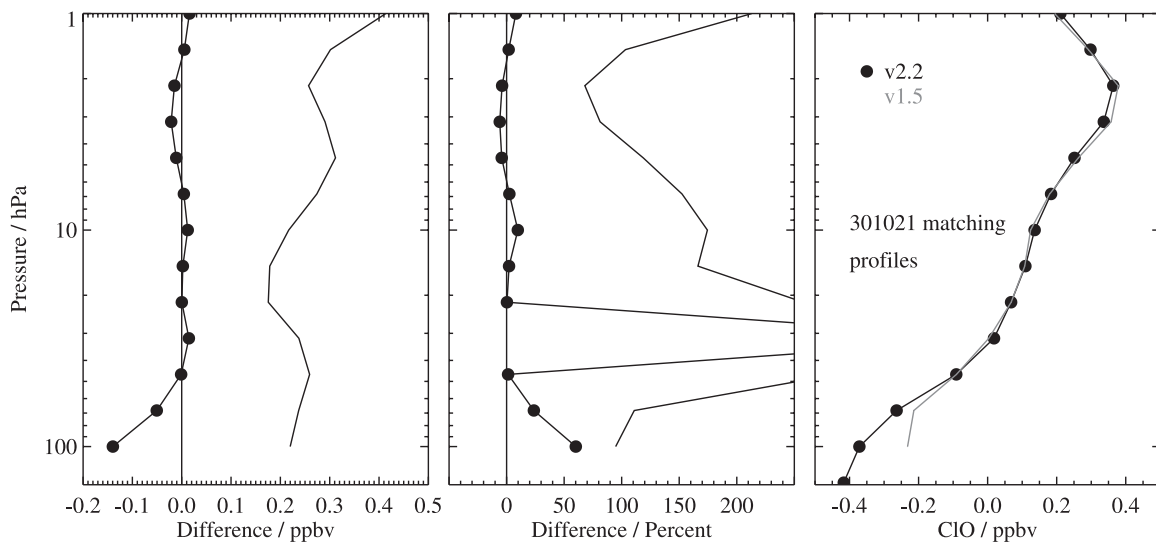


Figure 6. Comparison of v2.2 and v1.5 Aura MLS CIO measurements from 93 days for which both versions of data were available at the time of writing (February 2007). (left) Absolute differences ($v2.2 - v1.5$); the black line with dots (symbols indicate MLS retrieval surfaces) shows mean differences, and the solid black line shows the standard deviation of the differences. (middle) Same, for percent differences (computed relative to v1.5). Large percent differences at the 32 hPa retrieval level arise because CIO mixing ratios are very low in this region. (right) Global mean profiles for v2.2 (black, with dots) and v1.5 (grey). Note that the CIO retrieval has been extended down to 147 hPa in v2.2.

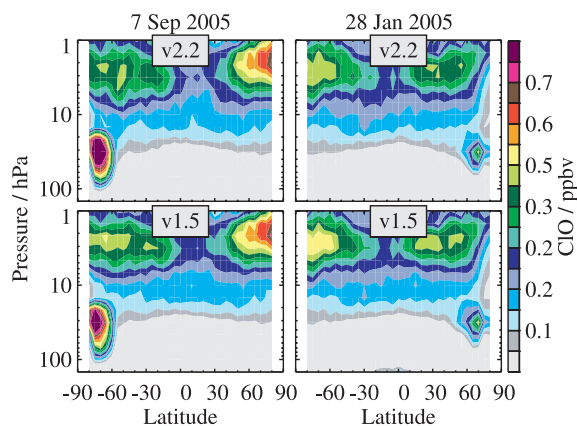


Figure 7. Zonal mean cross sections of (top) v2.2 and (bottom) v1.5 Aura MLS daytime (ascending) CIO for two selected days, chosen to illustrate CIO enhancement in the (left) southern (7 September 2005) and (right) northern (28 January 2005) winter polar regions.

[30] At the topmost level (not shown), nighttime mixing ratios are approximately zero at all EqLs and all seasons, except for a slight enhancement in the winter polar regions. At the levels below 660 K, however, a persistent negative bias is evident at low and middle latitudes, and at high latitudes outside winter. The magnitude of the bias in these regions is essentially the same in both daytime and nighttime mixing ratios, as expected since none of the potential sources of systematic uncertainty (see section 2.5) that could be giving rise to this bias are diurnally varying. The bias increases in magnitude at the lower levels, reaching ~ 0.3 – 0.4 ppbv at 460 K (Figure 8) and ~ 0.4 – 0.5 ppbv at 410 K (not shown). With the exception of the polar regions during winter, the bias exhibits only small variations with either season or latitude, and is essentially eliminated by taking ascending – descending (day – night) differences.

[31] At polar latitudes in both hemispheres, chlorine activation leads to substantial CIO enhancement during the winter. Figure 8 shows that the nighttime mixing ratios also exhibit nonnegligible positive values at this time, in some cases nearly as high as those observed during the day. It is well known from laboratory studies and in situ measurements that thermal decomposition of the CIO dimer, Cl_2O_2 , leads to increases in nighttime CIO abundances as temperatures increase over the range 190–215 K [e.g., Avallone and Toohey, 2001; World Meteorological Organization, 2007, and references therein]. Similar increases in nighttime CIO mixing ratios in the winter polar vortices with increasing temperature have been seen in satellite observations from UARS MLS [e.g., Waters *et al.*, 1993] and Michelson Interferometer for Passive Atmospheric Sounding (MIPAS) [Glatthor *et al.*, 2004], and CIO mixing ratios of 0.7–0.8 ppbv have been measured at night inside the Arctic vortex by Odin/SMR [Berthet *et al.*, 2005], with maximum nighttime CIO abundances observed in the regions of highest temperature.

[32] At the times/locations at which chlorine is not activated, the nighttime reservoir is ClONO_2 , and abundances of Cl_2O_2 are insignificant. In this case, the negative bias in the MLS CIO data can be eliminated by subtracting gridded

or zonal mean nighttime values from the individual daytime measurements. Figure 8, however, illustrates why taking day – night differences is not a practical approach inside the winter polar vortices: Subtraction of the nonnegligible nighttime CIO values substantially reduces the degree of chlorine activation indicated by the data. On the basis of a good correlation between MLS and SMR observations in the high-latitude lower stratosphere, with both instruments measuring the same mean CIO enhancement in the Antarctic spring vortex, Barret *et al.* [2006] speculated that the negative bias was absent in v1.5 MLS CIO for conditions of strong chlorine activation. No instrumental or retrieval issues suggest, however, that the bias should disappear when CIO is enhanced. We therefore believe that it is necessary to subtract an estimate of the bias from the individual measurements at each of the affected levels, whether or not CIO is enhanced.

[33] To determine the magnitude of the additive bias at each retrieval pressure level, we calculated daily averages of the CIO measurements in 20° -wide geographic latitude bins for which the solar zenith angle (SZA) is greater than 100° and the local solar time is between 2200 and 0400. To ensure that CIO was not enhanced, we restricted consideration to the days between 1 May and 1 November for the two northern high-latitude bins (50° – 70°N and 70° – 90°N) and to the days between 1 November and 1 May for the two southern high-latitude bins (50° – 70°S and 70° – 90°S). For the other latitude bands the calculations were performed for all 93 days (spanning all seasons) for which v2.2 measurements were available at the time of writing. The average of the daily mean values was then computed for each latitude band and pressure level. As shown in Figure 9, the bias in the CIO data worsens with increasing pressure. The dotted lines mark the magnitudes of the global mean biases estimated by averaging together the values for the individual latitude bins at each level, which are -0.04 , -0.14 , -0.31 , and -0.41 ppbv for the 32, 46, 68, and 100 hPa retrieval levels, respectively. No significant bias appears to be present in the data for the retrieval levels at or above 22 hPa. Figure 9 also shows, however, that the bias exhibits significant (up to 0.2 ppbv) latitudinal variation. In the lower stratosphere, CIO is mainly of interest in the winter polar regions, and using the global mean bias estimates, which are strongly influenced by the larger values at low latitudes, may lead to overcompensation. Thus for most analyses it is more appropriate to estimate the magnitude of the bias by including only the middle- and high-latitude bins in the averages (i.e., excluding the 30°S – 30°N region), leading to values of -0.02 , -0.12 , -0.27 , and -0.41 ppbv at 32, 46, 68, and 100 hPa, respectively (represented by the dashed lines in Figure 9). Further refinement in these bias estimates may be possible as more v2.2 CIO data become available, including better understanding of the latitudinal and/or seasonal dependencies of their magnitudes.

[34] The importance of accounting for the negative bias, especially in scientific studies examining CIO enhancement on potential temperature surfaces, is highlighted in Figure 10, which shows nighttime CIO measurements at 460 K as a function of temperature for representative days in the Arctic (Figure 10, top) and Antarctic (Figure 10, bottom) winters. In Figure 10 (left), in which the CIO data have not been corrected, the measurements appear to fall into two distinct

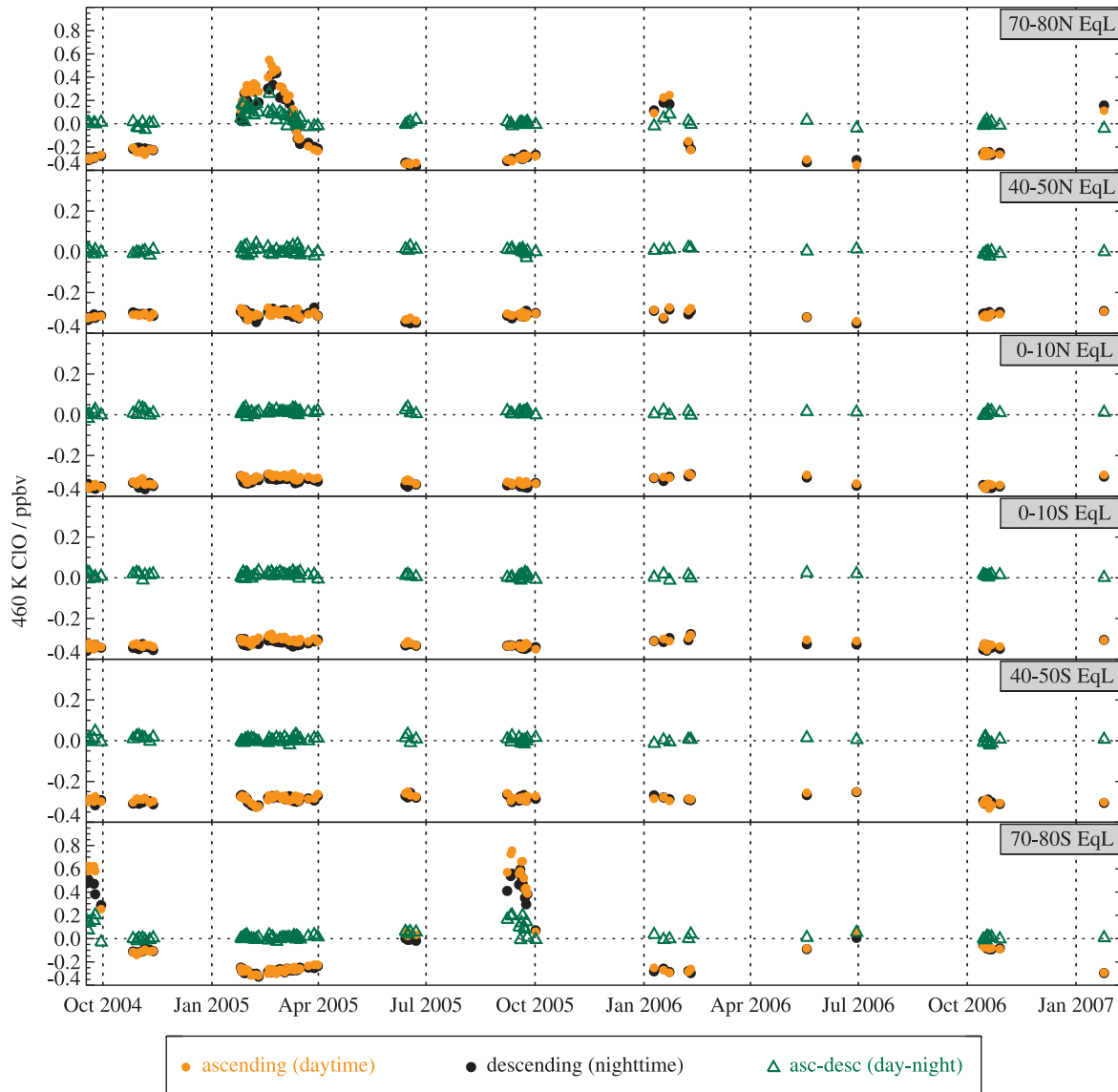


Figure 8. Time series of MLS v2.2 CIO measurements at 460 K potential temperature (corresponding to ~ 68 hPa, 17 km) for the 93 days processed at the time of writing. Temperatures from NASA’s Global Modeling and Assimilation Office Goddard Earth Observing System Version 4.0.3 (GEOS-4) were used to interpolate the data to potential temperature. Daily means were calculated by binning the measurements into 10° -wide equivalent latitude (EqL) bands and averaging; high, middle, and low EqL bands are shown for each hemisphere. Orange dots depict averages of data from the ascending (primarily daytime) side of the orbit, whereas black dots depict averages of data from the descending (primarily nighttime) side of the orbit. Differences of the daily ascending and descending averages (day – night) are shown with open green triangles. Note that the y axis ranges for the two high-latitude bins differ from those of the other bands.

populations, with the vortex (i.e., at high EqL in the winter hemisphere) data exhibiting little or no bias compared to data from outside the vortex. Interpretation of these plots is complicated by the fact that measurements from the 46-hPa retrieval surface, where the bias is smaller, are contributing to the values at 460 K inside the cold vortex, whereas measurements from the 68- and 100-hPa retrieval surfaces, where the bias is larger, are contributing to the values in the warmer extravortex regions. It is thus necessary to correct individual CIO measurements by subtracting the estimated negative bias at each of the affected retrieval levels before

interpolation to potential temperature surfaces, as shown in Figure 10 (right). The increase in nighttime high-EqL CIO with increasing temperature up to ~ 210 – 215 K is consistent with expectation as the equilibrium between CIO and its dimer shifts toward CIO and agrees well with the behavior seen in SMR measurements [Berthet *et al.*, 2005].

3. Comparison With UARS MLS Climatology

[35] The MLS on board UARS measured the global distribution of stratospheric CIO for much of the 1990s,

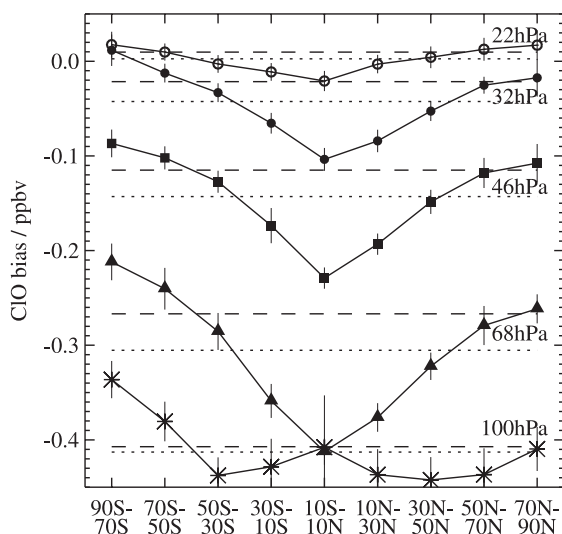


Figure 9. Estimates of the bias in MLS v2.2 CIO data in 20°-wide geographic latitude bands at 100, 68, 46, 32, and 22 hPa (labeled lines drawn with different symbols). Vertical error bars reflect the standard deviations in the averages of the daily mean values. The magnitudes of the global mean bias at each pressure level are denoted by the dotted lines; the dashed lines represent the average biases calculated using only the middle- and high-latitude bins (i.e., excluding the 30°S–30°N region).

albeit with approximately monthly gaps in high-latitude coverage arising from UARS yaw maneuvers and with significantly reduced temporal sampling in the latter half of the decade. A comprehensive overview of the seasonal, interannual, and interhemispheric variations in CIO in EqL bands throughout the lower stratosphere (420–700 K potential temperature) was produced from the UARS MLS data by *Santee et al.* [2003]. Taking a similar approach with Aura MLS measurements provides a means of quantitatively comparing to the CIO climatology derived from UARS MLS data. The daily means in Figure 11 were computed by binning both the UARS and the Aura MLS CIO measurements into 5° EqL bands and averaging; results are shown for 10 EqL bands over annual cycles in both hemispheres. All UARS MLS data collected from 1991 through 2000 are represented by grey dots. To illustrate the degree of interannual variability in the Aura MLS data record, the v1.5 CIO measurements obtained in each year since launch in July 2004 are depicted in different shades of blue, with results from the v2.2 retrievals performed to date overlaid in red. Note that neither the v1.5 nor the v2.2 Aura MLS data have been corrected for the negative bias described in section 2.7. Data from both MLS instruments have been interpolated to the 520 K potential temperature surface (~46 hPa, 19 km) near the peak in the CIO vertical profile, using temperatures from the U.K. Met Office analyses [*Swinbank et al.*, 2002] for UARS MLS and from NASA’s Global Modeling and Assimilation Office Goddard Earth Observing System Version 4.0.3 (GEOS-4) [*Bloom et al.*, 2005] for Aura MLS.

[36] Both the latitudinal variation of CIO and its evolution over an annual cycle match those in the climatology based on the multiyear UARS MLS data set. Figure 11, however,

clearly shows the pervasive low bias in both the v1.5 and the v2.2 Aura MLS CIO measurements in the lower stratosphere (compare the grey dots with the red and blue dots). Equivalent latitude means of CIO at other levels throughout the middle and upper stratosphere (not shown) indicate excellent agreement on average with the climatological values, but, as seen also in Figure 11, much less scatter is present in the v2.2 data than in the corresponding UARS MLS measurements.

4. Comparisons With Other Observations

[37] In this section the accuracy of the Aura MLS v2.2 CIO measurements is assessed through comparisons with correlative data sets from a variety of different platforms, some of which were acquired in dedicated Aura validation campaigns. For most of these comparisons we use the traditional approach of considering matched pairs of profiles that are closely collocated both geographically and temporally. The coincidence criteria used to select the matches vary and are stated in each subsection below. In some cases, use of an additional filter based on the potential vorticity of the profiles (to ensure that only meteorologically consistent air masses are compared) was explored but was found to have little impact on the average differences.

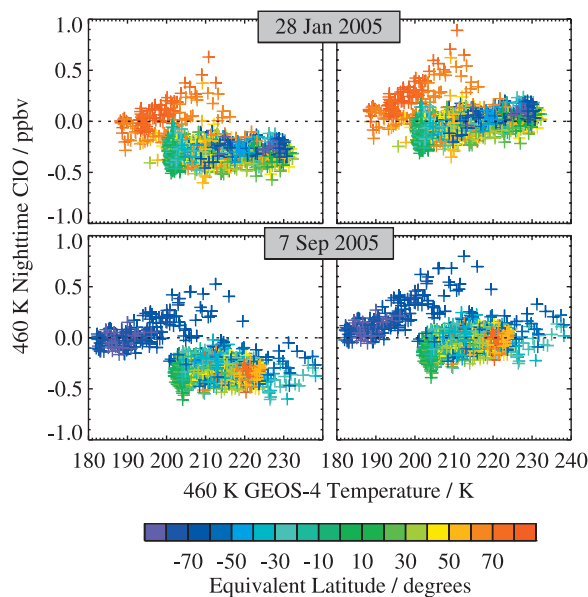
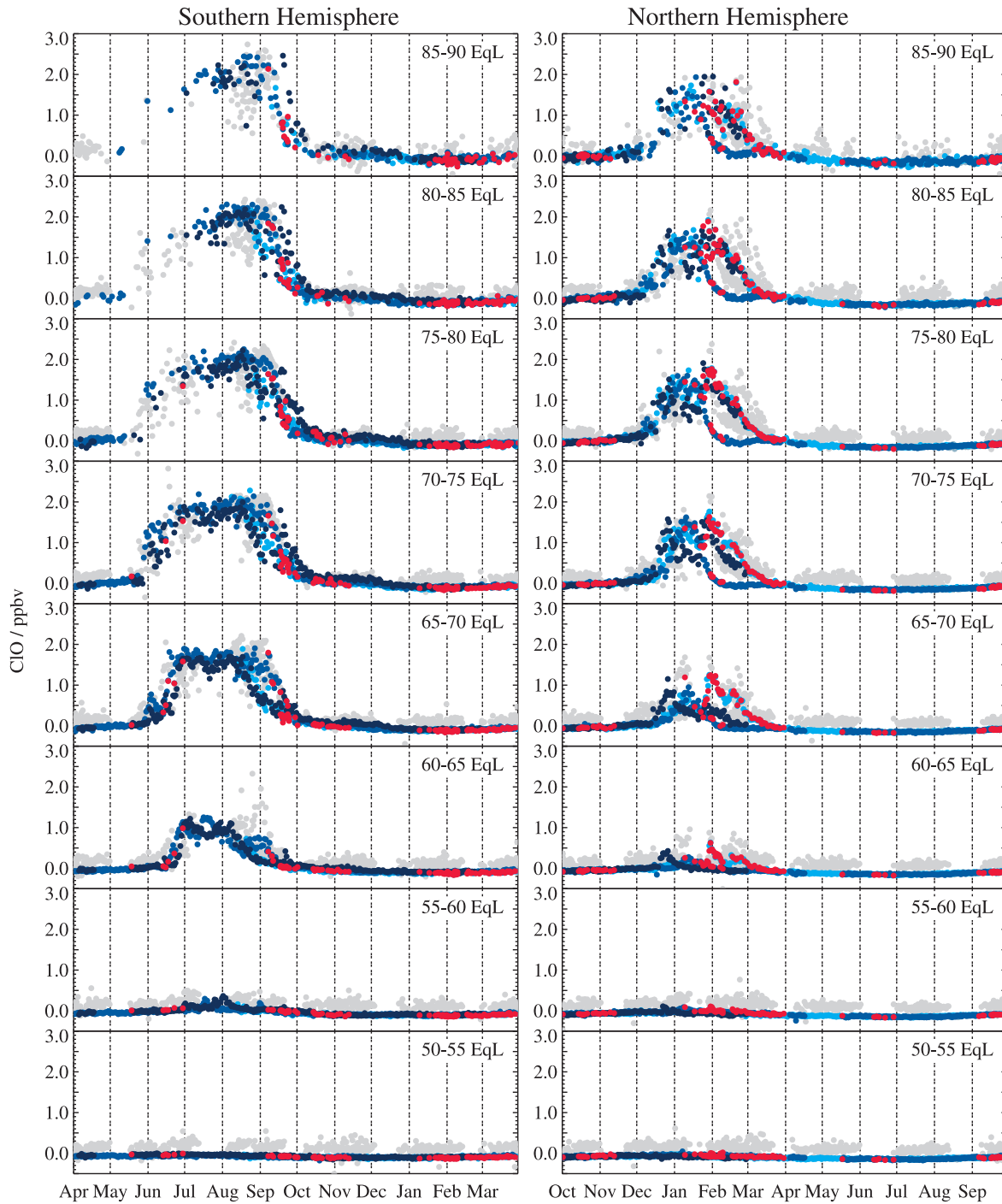


Figure 10. MLS v2.2 nighttime (solar zenith angle (SZA) >100°, local solar time (LST) between 2200 and 0400) CIO measurements at 460 K as a function of GEOS-4 temperature for two representative days during (top) northern (28 January 2005) and (bottom) southern (7 September 2005) winter. Data points are color-coded by equivalent latitude. (left) Uncorrected MLS data and (right) corrected data, for which the estimate of the bias (based on the middle- and high-latitude values; dashed lines in Figure 9) has been subtracted from the individual “raw” mixing ratios at each affected retrieval pressure level prior to interpolation to potential temperature.



UARS Aura v1.5 (2003-2004 2004-2005 2005-2006 2006-2007) v2.2

Figure 11. Time series of MLS ClO measurements at 520 K potential temperature (corresponding to ~46 hPa, 19 km) for the (left) Southern and (right) Northern Hemispheres. Daily means were calculated by binning the measurements into 5°-wide EqL bands and averaging. Grey dots depict version 5 UARS MLS ClO data taken over the period 1991–2000; blue dots depict v1.5 Aura MLS ClO data, with different shades of blue representing different years as indicated in the legend, and red dots depict v2.2 Aura MLS data for the 93 days processed at the time of writing. Only daytime data were included in the averages ($SZA < 92^\circ$, $1000 < LST < 1500$). Dashed vertical lines demark calendar months.

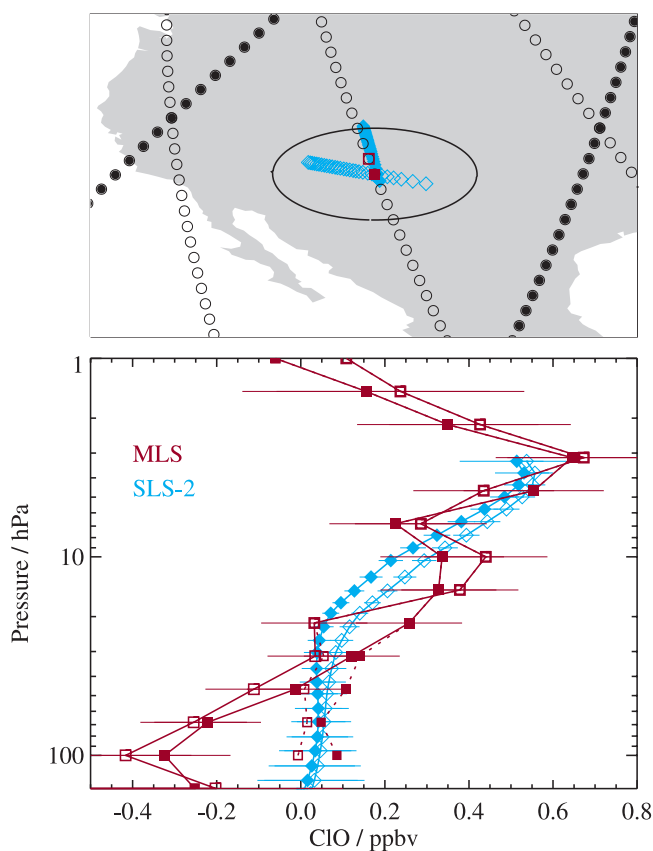


Figure 12. (top) Path traversed by measurements from the balloon-borne SLS-2 instrument (cyan diamonds) during the flight from Fort Sumner, NM, on 20–21 September 2005. Measurement tracks from nearby MLS ascending (daytime, open circles) and descending (nighttime, solid circles) orbit legs are also shown. The two MLS data points closest to the balloon measurements geographically and temporally are indicated by red squares, with the closer one denoted by a solid symbol; the 500-km radius around the closest MLS point is overlaid in black. (bottom) Profiles of CIO, corresponding to the symbols in the top image, from MLS (red squares; solid lines with larger symbols show “raw” MLS data, dotted lines with smaller symbols show MLS data corrected for the negative bias as described in section 2.7) and SLS-2 (cyan open and solid diamonds). Error bars represent the estimated precisions of each instrument, taken from the data files (for clarity, they have been omitted from the corrected MLS profiles).

4.1. Ground-Based Measurements

[38] Long-term monitoring of stratospheric CIO has been provided by ground-based millimeter-wave spectrometers operating at Mauna Kea, Hawaii (20°N) [Solomon *et al.*, 2006] and Scott Base, Antarctica (77.85°S) [Solomon *et al.*, 2000, 2002]. The instruments, which are notionally identical, measure the CIO emission line at 278.6 GHz to derive profiles of CIO between 15–20 and 40 km with precision and accuracy each ~ 0.1 ppbv; vertical resolution is ~ 10 km, although the height of the peak is determined to an accuracy of ± 1.5 km [Solomon *et al.*, 2000].

[39] Measurements of CIO from the Scott Base instrument are compared to Aura MLS data from nearby overpasses in a companion paper by Connor *et al.* [2007]; their analysis is summarized briefly here. The intercomparisons cover the period of peak chlorine activation in September 2005, with measurements from 16 days passing all weather, quality control, and coincidence criteria during this interval. The ground-based data are made by subtraction of the nighttime signal from the daytime measurements, which are selected to be within 30 min of the time of the MLS ascending node overpass (approximately 1700 local solar time at this latitude); the MLS data are ascending – descending differences, typically within ~ 100 km of the Scott Base instrument’s beam in the lower stratosphere. Note that because day – night differences are used for both data sets, these comparisons provide no insight into the magnitude of the bias in the MLS CIO data. The analysis accounts for the influence of the a priori on the ground-based measurements and their coarser vertical resolution by simulating “convolved” MLS profiles. In this approach, the MLS data are assumed to represent the real atmosphere, and microwave spectra calculated from them are then run through the same data processing system used for the ground-based measurements. Both v1.5 and a smaller subset of v2.2 MLS CIO data are examined; mean differences with the Scott Base values are nearly identical for the two MLS data versions. The shapes of the retrieved Scott Base and convolved MLS profiles are very similar; in particular, both the amplitude and the altitude of the secondary peak in the CIO profile in the upper stratosphere are in excellent agreement in the two data sets. The mean difference in the amplitude of the lower stratospheric peak (Scott Base–simulated MLS) is 0.10 ± 0.07 ppbv ($11 \pm 8\%$); that is, the convolved MLS CIO values are on average marginally smaller than the Scott Base values. The mean difference is not statistically significant, however, and day-to-day variability is large, so some of the disagreement may be attributable to real horizontal variations in the CIO distribution in this region.

4.2. Balloon Measurements

[40] As part of the Aura validation effort, measurements of CIO were obtained near Aura overpasses from the JPL Submillimeterwave Limb Sounder-2 (SLS-2) during a balloon campaign carried out from Fort Sumner, New Mexico, in September 2005. SLS-2 is a high-resolution heterodyne radiometer-spectrometer that measures limb thermal emission spectra of several species, including CIO, at frequencies near 650 GHz. A previous version of the instrument was described by Stachnik *et al.* [1999]; the newer SLS-2 incorporates an LHe-cooled superconductor insulator superconductor (SIS) quasi-optic mixer that has greater than 20 times the radiometric sensitivity of the earlier Schottky mixer instrument (system temperature T_{sys} of ~ 250 K double-sideband compared to ~ 5500 K). Vertical resolution of the SLS-2 data is roughly 2–3 km below the balloon float altitude (~ 35 km) and 5–6 km above.

[41] Comparisons between the balloon measurements and coincident MLS measurements are shown in Figure 12, where the MLS profiles are within 1° of latitude, 12° of longitude, and 4 h of the balloon measurements. Good agreement is seen in the upper stratosphere, in terms of both the altitude and the approximate magnitude of the

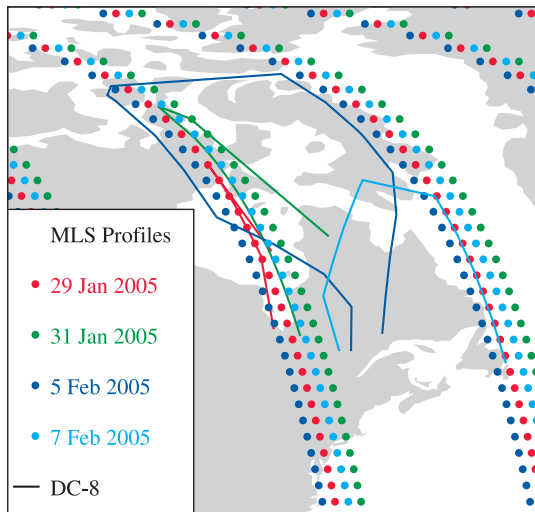


Figure 13. Flight tracks (lines color-coded by date) of the NASA DC-8 aircraft during the Polar Aura Validation Experiment (PAVE) mission conducted from Portsmouth, New Hampshire, in January/February 2005. Only flights on days for which both MLS v2.2 and ASUR data are available are shown. The MLS ground tracks on these days are indicated by solid dots in corresponding colors.

high-altitude peak. In the lower stratosphere, the significant negative bias in the MLS CIO retrievals below 32 hPa is evident. Correcting for this bias by subtracting its estimated value at each of the affected retrieval levels (section 2.7)

leads to much better agreement, well within the combined error bars.

4.3. Aircraft Measurements

4.3.1. ASUR

[42] Several aircraft campaigns have been conducted since the launch of Aura; although they have had strong science components, a significant focus of some of these campaigns has also been to collect observations to assist in the validation of Aura measurements. During one of these campaigns, the Polar Aura Validation Experiment (PAVE) in January/February 2005, the Airborne SUBmillimeter Radiometer (ASUR) made remote sensing measurements of CIO on flights of the NASA DC-8 research aircraft within and on the edge of the Arctic polar vortex (see especially *Kleinböhl et al. [2005, auxiliary material]*). Flights were coordinated to align along Aura instrument ground tracks near the time of the satellite overpass, as illustrated in Figure 13; note, however, that some of these flights were targeted toward validation of data from other Aura instruments, and in these cases the aircraft flight tracks are offset from those of MLS. ASUR is a passive heterodyne instrument that measures CIO using the cluster of lines at 649.5 GHz; more information on the ASUR measurement and retrieval system is given by *Kleinböhl et al. [2002]*. Along with other stratospheric trace gases, vertical profiles of CIO are retrieved from spectrally resolved pressure-broadened emission lines with a vertical resolution of 5–10 km calculated on a 2 km vertical grid over the range from

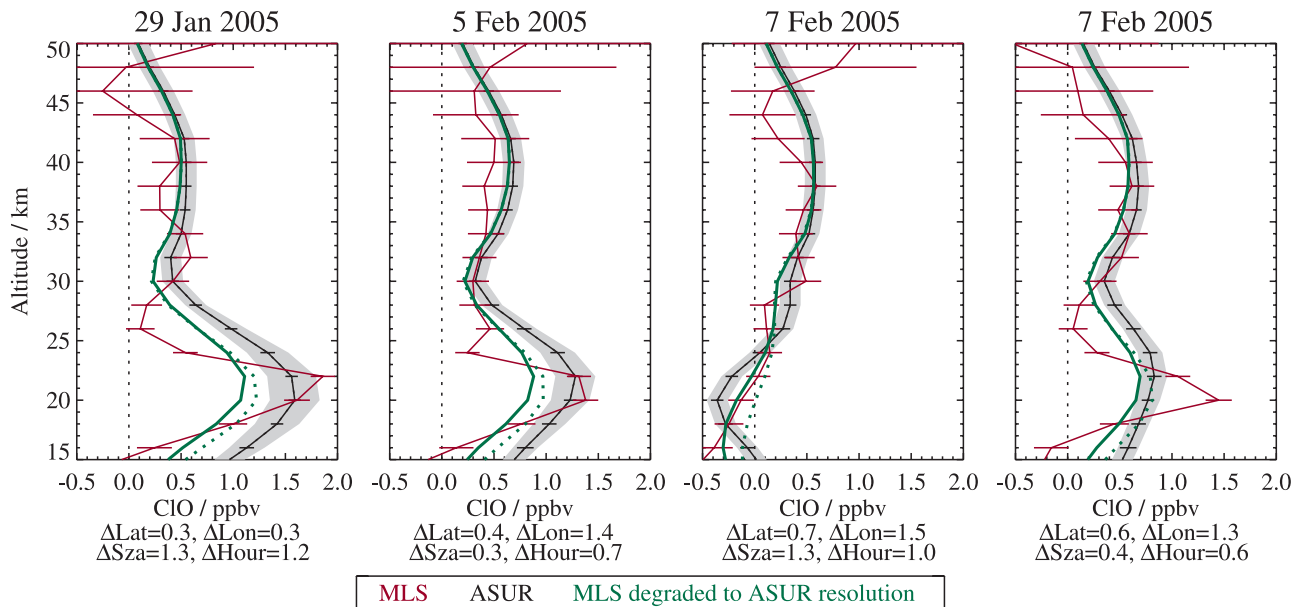


Figure 14. Comparison of the closest MLS v2.2 CIO profiles to the ASUR measurements taken along Aura overpasses during the PAVE campaign in January/February 2005; individual panels show four representative comparisons from three flights. ASUR profiles are shown in black, with grey shading indicating the accuracy and error bars indicating the 1- σ statistical error, derived from the measurement noise. MLS profiles are shown in red, with error bars representing the estimated precision of the CIO data reported by the retrieval system. MLS profiles multiplied by the ASUR averaging kernels are shown in green; solid lines show “raw” MLS CIO values, dotted lines show MLS data corrected for the negative bias as described in section 2.7. The separation between the MLS and ASUR profiles in latitude, longitude, time, and solar zenith angle is noted for each case.

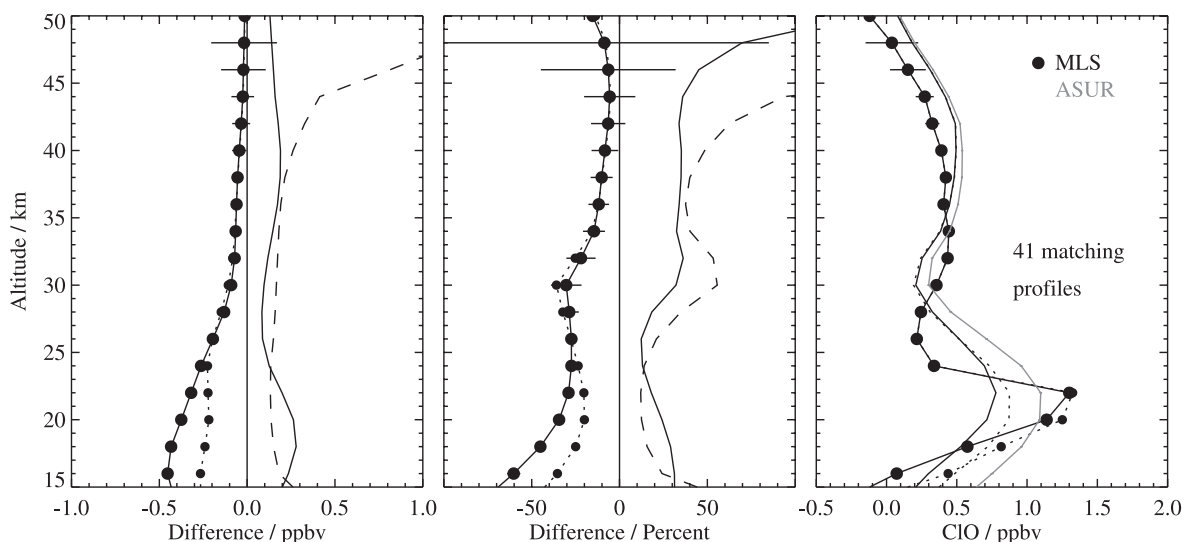


Figure 15. Summary of comparisons of coincident MLS v2.2 and ASUR CIO profiles. (left) Absolute differences (MLS – ASUR, where the MLS data have been interpolated onto the ASUR grid and multiplied by the ASUR averaging kernels); the solid line with large dots shows mean differences with the “raw” MLS data, and the dotted line with small dots shows mean differences with the MLS data corrected for the negative bias as described in section 2.7. The solid line (with no symbols) shows the standard deviation about the mean differences, and the dashed line shows the root sum square of the theoretical precisions of the two data sets. (middle) Same, for percent differences, where percentages have been calculated by dividing the mean differences by the mean ASUR values at each surface. (right) Mean profiles for MLS (solid line with large dots for “raw” MLS data, dotted line with small dots for corrected MLS data), MLS multiplied by the ASUR averaging kernels (solid line with no symbols for “raw” MLS data, dotted line with no symbols for corrected MLS data), and ASUR (grey).

~15 to 50 km. The accuracy of the CIO measurements is estimated to be ~10% or 0.15 ppbv, whichever is higher.

[43] Figures 14 and 15 compare the closest v2.2 MLS profiles to ASUR profiles obtained along Aura overpasses during PAVE (coincidence criteria: $\pm 2^\circ$ latitude, $\pm 4^\circ$ longitude, ± 2 h); all comparisons are of profiles obtained in daylight. Figure 14 shows a few representative CIO profiles from three of the PAVE flights, selected to illustrate unenhanced, moderately enhanced, and strongly enhanced conditions. MLS, with considerably better vertical resolution, observes a much more sharply defined peak in CIO in the lower stratosphere than does ASUR. To account for the differing vertical resolutions of the two data sets, in Figure 14 we also show results from applying the ASUR averaging kernels to the MLS data; in general, degrading the resolution of the MLS CIO measurements in this manner significantly improves the comparisons. Agreement is typically good near the secondary peak in the upper stratosphere, with average differences (Figure 15) between the MLS profiles multiplied by the ASUR averaging kernels and the ASUR profiles less than 0.1 ppbv (10%), well within the combined uncertainties in the two instruments. The smoothed MLS profiles have smaller maximum abundances in the lower stratosphere, however, with average differences increasing below 30 km to greater than 0.4 ppbv (60%). The disparity between the two measurements in the lower stratosphere is significantly reduced but not eliminated when the negative bias in the v2.2 MLS CIO measurements is corrected.

4.3.2. HALOX

[44] In situ measurements of highly enhanced CIO were made by the HALOX instrument on board the stratospheric research aircraft M55 Geophysica during a flight inside the Arctic polar vortex on 7 March 2005 [see also *von Hobe et al.*, 2006, auxiliary material], just prior to the major final warming. A detailed description of the HALOX instrument, which employs the chemical conversion resonance fluorescence technique to measure CIO, is provided by *von Hobe et al.* [2005]. CIO is measured with a time resolution of 10 s, a detection limit of 5 ppt, and an accuracy of ~15%.

[45] Using HALOX data for MLS validation purposes raises the issue of how to meaningfully compare the considerably coarser-resolution and less precise satellite measurements, which represent “average” conditions over a relatively large volume of air, with the highly precise in situ measurements, which represent conditions at a local point. Geophysical variability inevitably complicates interpretation of the comparison of data sets having sampling volumes of such vastly different scales. Furthermore, since the HALOX data were not obtained as part of a coordinated Aura validation program, coincident measurements are limited. In the analysis presented here, trajectory calculations have been used to map the air masses measured by HALOX to their locations at the time of the MLS overpasses; the closest coincidences between MLS and HALOX (advected to the MLS measurement times) occur on the ascent and dive segments of the flight (Figure 16a). Although both data sets represent daytime conditions, the

HALOX data were obtained earlier in the morning at slightly higher SZAs (Figure 16b).

[46] In Figure 16 we take a qualitative approach in which the in situ measurements are overlaid on the MLS CIO field geographically closest to the Geophysica flight track. Figure 16c shows the comparisons with the “raw” v2.2 MLS CIO data; in Figure 16d the bias correction described in section 2.7 has been applied to the MLS data. Results are generally encouraging, especially at the lowest retrieval levels. HALOX frequently senses fine-scale structure not observable by MLS, but for the most part the spatial trends are roughly in agreement. MLS mixing ratios, however, are considerably lower than those recorded by HALOX at the highest altitudes (lowest pressures) attained by the

Geophysica, even after the negative bias in the MLS data has been accounted for (Figure 16d).

[47] The qualitative comparisons in Figure 16 are hampered by the disparities in sampling and resolution between the two instruments. As discussed by *Livesey et al.* [2007], proper comparison of MLS and in situ measurements involves a two-step process: the high-resolution in situ data are first downsampled to the MLS retrieval grid using a least squares fit, and the smoothed data are then multiplied by the MLS averaging kernels. This kind of quantitative comparison is shown for the separate flight segments in Figure 17. After conversion to the coarse-resolution MLS grid, the HALOX measurements obtained during ascent (blue) match the coincident bias-corrected MLS profile to within 0.1 ppbv (15%) at 100 hPa, although lack of high-altitude HALOX measurements during this flight leg increases the uncertainty of the smoothed value at this level. The dive (red) provided close coincidences with two MLS profiles, which show excellent agreement (within ~5%) at 100 hPa. At 68 hPa, however, HALOX sees ~0.25 ppbv (~15–20%) more CIO than indicated by MLS. This degree of agreement is within the combined accuracies of the two instruments.

4.4. Satellite Measurements

[48] Satellite measurements provide the opportunity for more spatially and temporally extensive intercomparisons than those with ground-based, balloon, or aircraft data sets. They are also typically well matched to the MLS horizontal and vertical resolution. CIO is retrieved from spectra measured by MIPAS on board the European Space Agency Environmental Satellite (Envisat), but, although these data

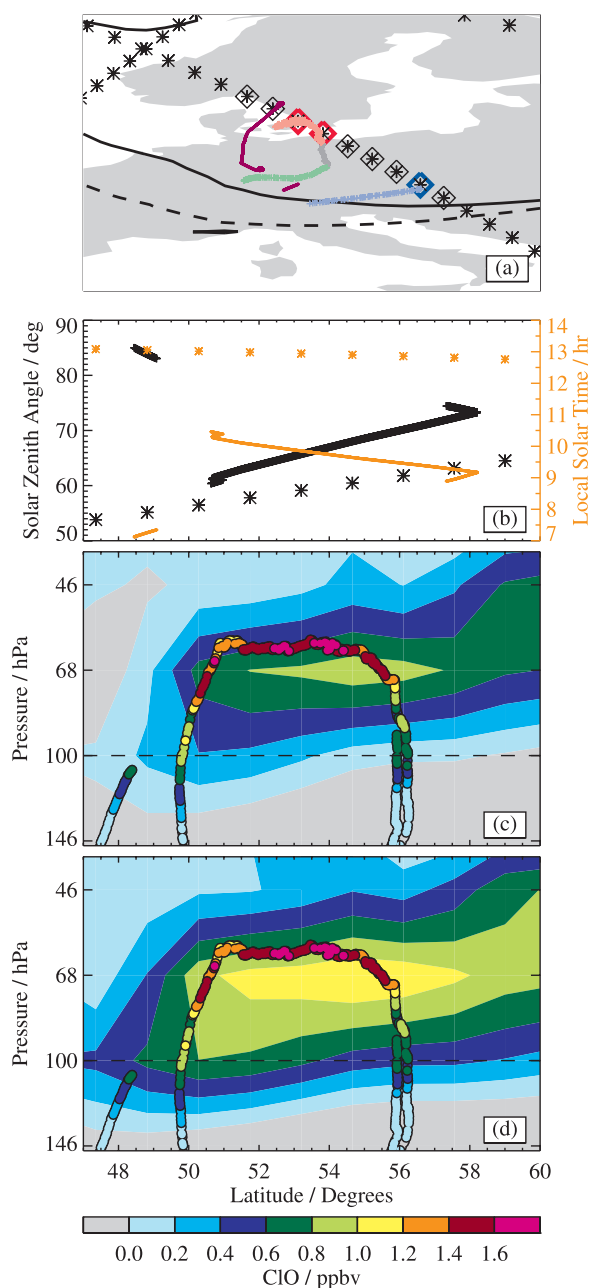


Figure 16. (a) Flight track (dark magenta) of the M55 Geophysica aircraft inside the Arctic polar vortex over Europe on 7 March 2005. Nearby MLS ground tracks on this day are denoted by asterisks; the specific MLS measurement points displayed in the contour plots of Figures 16c and 16d are highlighted with diamonds, and the three MLS profiles shown in Figure 17 are outlined in blue and red. The position of the HALOX flight path shifted to the time of the MLS overpass using trajectory calculations based on European Centre for Medium-Range Weather Forecast (ECMWF) reanalyses are also shown (small plus signs), color-coded for different flight segments: ascent (pale blue), dive (pale red), level flight on return leg (grey) and descent (pale green). Overlaid in black are contours of GEOS-4 PV representative of the vortex edge at 410 K (solid line) and 460 K (dashed line), corresponding to the MLS retrieval levels at 100 and 68 hPa, respectively. (b) Solar zenith angle (large black symbols) and local solar time (small orange symbols) for the MLS (asterisks) and HALOX (plus signs) measurements. (c) V2.2 MLS CIO (contours) for the measurement points indicated in Figure 16a. The dashed line at 100 hPa signifies that the MLS data below this level are not considered reliable for scientific studies. Overlaid (solid circles) are the HALOX CIO measurements. (d) As in Figure 16c but with the bias correction described in section 2.7 applied to the MLS CIO measurements.

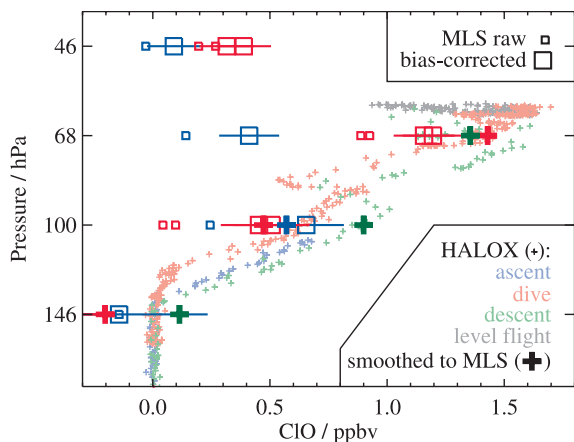


Figure 17. Three profiles of MLS CIO, color-coded as in Figure 16a, where small boxes show “raw” MLS values and large boxes show bias-corrected values (note that no bias correction is performed at 147 hPa, as the MLS CIO data are not deemed reliable for scientific use at this level). Error bars on corrected MLS points represent estimated precision. Also shown are HALOX measurements from the ascent, dive, level flight, and descent flight segments (small plus signs), color-coded as in Figure 16a, and the corresponding least-squares interpolation of the HALOX data multiplied by the MLS averaging kernels (see text; large plus signs in darker shades). Because of the shape of the MLS averaging kernel at 147 hPa (see Figure 3), to achieve proper smoothing at that level in situ data must be available up to at least 68 hPa; lack of high-altitude HALOX data during ascent (blue symbols) thus precludes conversion to the MLS grid at either 68 or 147 hPa.

have been presented for specific studies [Glatthor *et al.*, 2004; von Clarmann *et al.*, 2005], they are not readily available. The Atmospheric Chemistry Experiment Fourier Transform Spectrometer (ACE-FTS) on the Canadian Space Agency’s SCISAT-1 mission also measures CIO, but these data remain a research product requiring special handling at this time [Dufour *et al.*, 2006; K. Walker, personal communication, 2005]. Therefore, we restrict our attention to comparisons with CIO measured by the SMR instrument on board the Swedish-led Odin satellite [Murtagh *et al.*, 2002].

[49] Odin was launched in February 2001 into a near-polar, sun-synchronous, ~600-km altitude orbit with an 1800 LT ascending node. Odin operates in a time-sharing arrangement, alternating between astronomy and aeronomy modes; SMR observes limb thermal emission from CIO on roughly two measurement days per week using an autocorrelator spectrometer centered at 501.8 GHz. Operational Level 2 CIO retrievals are produced by the Chalmers University of Technology (Göteborg, Sweden). Retrievals from a similar data processing system in France were compared to MLS v1.5 CIO measurements by Barret *et al.* [2006]. The retrieval methodology and error characterization for the Chalmers version 1.2 data, and the differences between the French and Swedish data processing systems, are described in detail by Urban *et al.* [2005]. The main differences between the Chalmers versions 1.2

and 2.0 are summarized by Urban *et al.* [2006]. Here we use Chalmers version 2.1 data, which for CIO are very similar to those in version 2.0, with differences typically smaller than ~50 pptv. The Chalmers version 2.0 CIO data have horizontal resolution of ~300–600 km, vertical resolution of 2.5–3 km, and single-scan precision better than 0.15 ppbv over the range from 15 to 50 km [Urban *et al.*, 2005, 2006]; similar values apply for the version 2.1 CIO

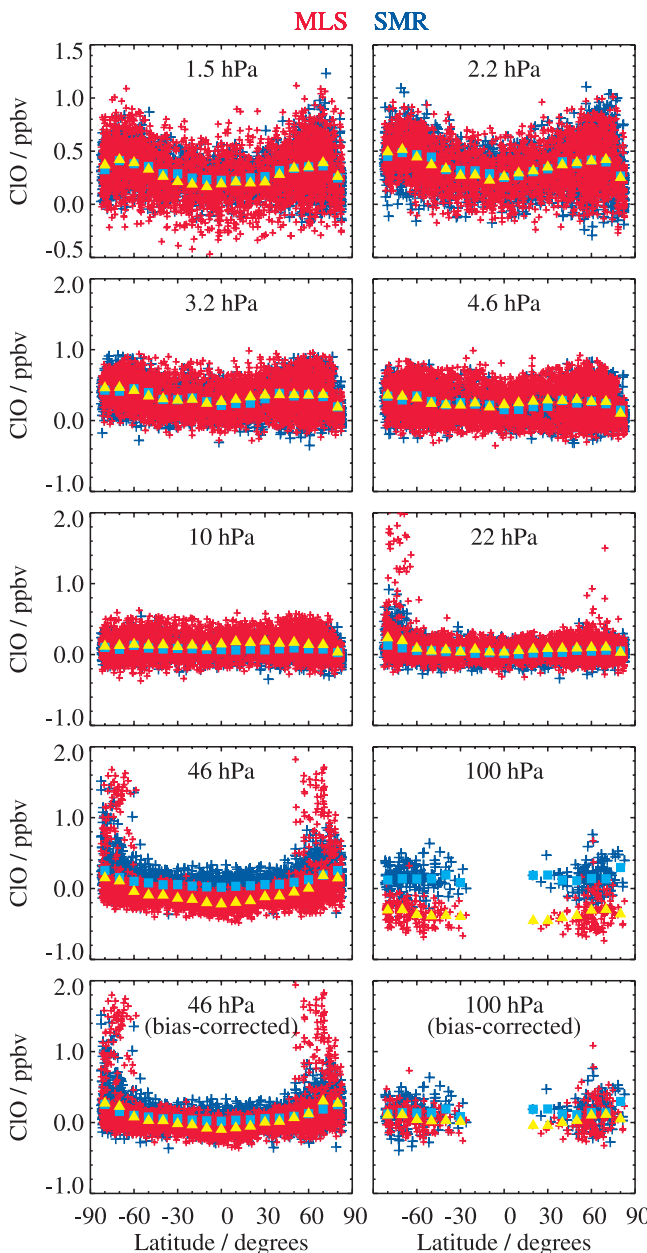


Figure 18. Scatterplot of coincident CIO profiles from “raw” MLS v2.2 data (red) and Odin/SMR Chalmers version 2.1 data (blue, see text), as a function of latitude for eight selected retrieval surfaces. Overplotted are the zonal mean values calculated in 10°-wide latitude bands for both the MLS (yellow triangles) and SMR (cyan squares) data. The 46 and 100 hPa comparisons are repeated (bottom row) using the bias-corrected MLS CIO data.

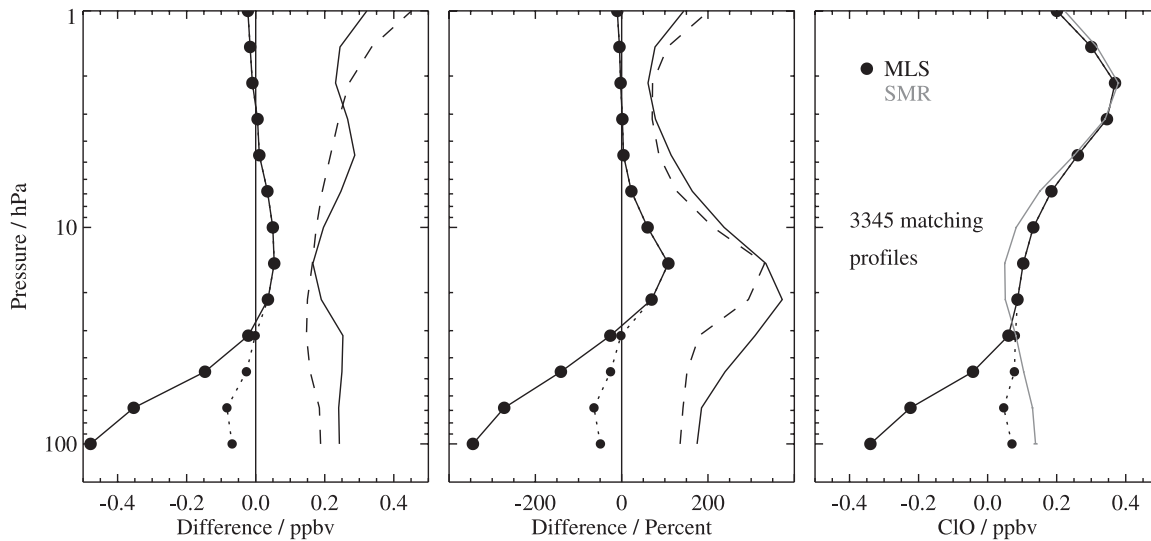


Figure 19. Comparison of coincident CIO profiles from MLS v2.2 data and Odin/SMR Chalmers version 2.1 data. (left) Absolute differences (MLS – SMR); the solid line with large dots (symbols indicate MLS retrieval surfaces) shows mean differences with the “raw” MLS data, and the dotted line with small dots shows mean differences with the MLS data corrected for the negative bias as described in section 2.7. The solid line (with no symbols) shows the standard deviation about the mean differences, and the dashed line shows the root sum square of the theoretical precisions of the two data sets. (middle) Same, for percent differences, where percentages have been calculated by dividing the mean differences by the global mean SMR value at each surface. (right) Global mean profiles for MLS (solid line with large dots for “raw” MLS data, dotted line with small dots for corrected MLS data) and SMR (grey).

data. The estimated total systematic error is less than 0.1 ppbv throughout the vertical range [Urban *et al.*, 2005, 2006]. Only good quality SMR data points are included in these comparisons (i.e., assigned flag QUALITY = 0, and a measurement response for each retrieved mixing ratio larger than 0.75 to ensure that the information has been derived from the measurements, with a negligible contribution from

the climatological a priori profile [Urban *et al.*, 2005; Barret *et al.*, 2006]).

[50] Figures 18 and 19 compare all coincident profiles obtained within $\pm 1^\circ$ in latitude, $\pm 4^\circ$ in longitude, and ± 12 h from 49 days for which both SMR and v2.2 MLS data are available. All seasons are represented in this set of comparison days. Because the vertical resolution of the SMR CIO measurements is similar to that of the Aura MLS CIO

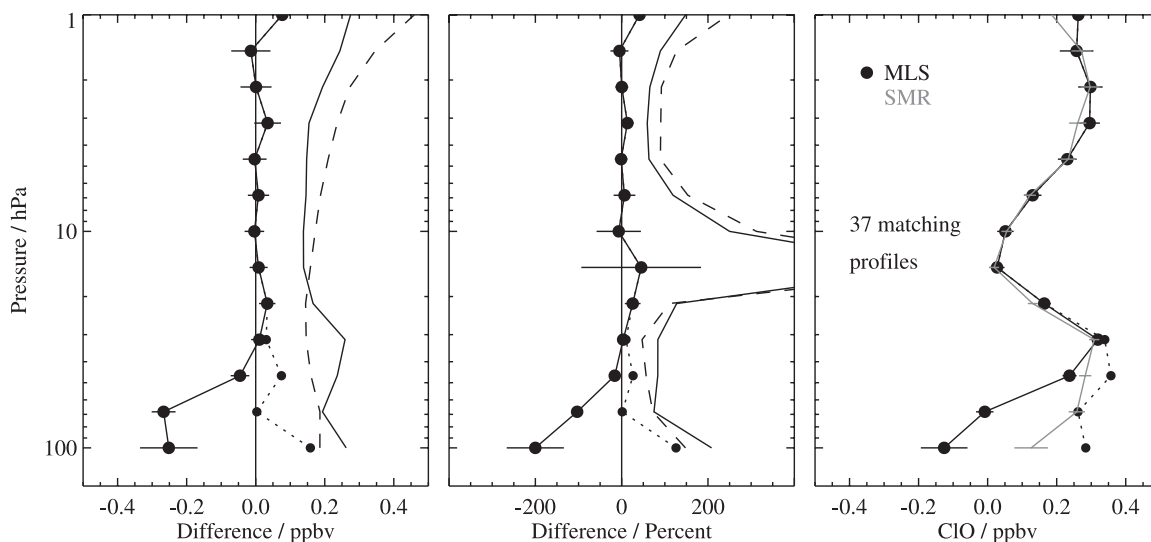


Figure 20. As in Figure 19, with additional SZA and LST coincidence criteria imposed (see text).

Table 2. Summary of Aura MLS v2.2 CIO Characteristics

Pressure, hPa	Resolution Vertical × Horizontal, ^a km	Precision, ^b ppbv	Bias Uncertainty, ^c ppbv	Scaling Uncertainty, ^c %	Known Artifacts or Other Comments
0.68–0.001	–	–	–	–	unsuitable for scientific use
1.0	3.5 × 350	±0.3	±0.05	±15%	
22–1.5	3–4.5 × 250–400	±0.1	±0.05	±5–15%	
32	3 × 400	±0.1	±0.1	±10%	–0.02 ppbv systematic bias ^d
46	3 × 450	±0.1	±0.1	±20%	–0.12 ppbv systematic bias ^d
68	3 × 500	±0.1	±0.1	±20%	–0.27 ppbv systematic bias ^d
100	3.5 × 500	±0.1	±0.1	±20%	–0.41 ppbv systematic bias ^d
147–316	–	–	–	–	unsuitable for scientific use
1000–464	–	–	–	–	not retrieved

^aHorizontal resolution in along-track direction; cross-track resolution is ~ 3 km, and the separation between adjacent retrieved profiles along the measurement track is 1.5° great circle angle (~ 165 km).

^bPrecision on individual profiles, determined from observed scatter in nighttime (descending) data in a region of minimal atmospheric variability.

^cValues should be interpreted as $2\text{-}\sigma$ estimates of the probable magnitude and, at the higher pressures, are the uncertainties after subtraction of the known negative bias tabulated in the rightmost column.

^dDetermined directly from the observations, not from simulations. Values quoted are based on averages over middle and high latitudes; see section 2.7 for latitudinal variations in the magnitude of the bias estimates.

measurements, for these comparisons the SMR profiles have been linearly interpolated in log-pressure to the fixed MLS retrieval pressure surfaces. The scatterplots of Figure 18 indicate good agreement in the general morphology of the CIO distribution, although the MLS data indicate stronger enhancements in the polar regions, particularly in the north; this apparent disparity is most likely related to solar zenith angle and local solar time differences between the matched profiles. The large negative bias in the MLS retrievals is evident in the comparisons at the lowest levels, with average differences between MLS and SMR CIO exceeding 0.45 ppbv at 100 hPa (Figure 19). The discrepancy between the two measurements in the lower stratosphere is significantly reduced but not eliminated when the negative bias in the v2.2 MLS CIO measurements is corrected. A possible high bias of 0.1–0.2 ppbv in the SMR lower stratospheric measurements obtained outside the vortex during nighttime, when CIO abundances fall below the detection limit of the instrument [Berthet *et al.*, 2005], may largely explain the remaining offset. Differences are typically within ~ 0.05 ppbv at and above 32 hPa, with MLS values larger through most of this region; because of the very low mixing ratios, however, these values correspond to percent differences larger than 100% at some levels. As with the ground-based measurements, the amplitude and the altitude of the peak in the upper stratosphere are matched well.

[51] The analysis presented in Figures 18 and 19 takes no account of the differences in solar zenith angle in the two CIO data sets. Barret *et al.* [2006] estimated that a 2° increase in SZA roughly corresponds to a 0.1 ppbv decrease in CIO, on the order of the estimated single-scan precision of the measurements; they concluded that a SZA coincidence criterion of $\pm 2^\circ$ is appropriate for an intercomparison of the CIO measurements from MLS and SMR. Because of differences in the observational patterns of the two instruments (both in sun-synchronous orbits), measurement points satisfying this SZA filter occur only at the highest latitudes, poleward of 70° in both hemispheres. In Figure 20 we summarize the comparison results obtained by imposing the additional SZA criterion and tightening the local solar

time criterion to ± 2 h. Such stringent coincidence criteria greatly reduce the number of matched points but significantly improve the agreement between the two data sets, with differences less than 0.05 ppbv (corresponding to $\sim 10\text{--}30\%$ over most of the profile) everywhere except at the bottom two levels, where the negative bias in the MLS data is largest. Correcting for the MLS bias enhances the agreement, although the results indicate that MLS actually overestimates CIO relative to SMR by more than 0.15 ppbv at 100 hPa.

5. Summary and Conclusions

[52] We have assessed the quality and reliability of the Aura MLS version 2.2 (v2.2) CIO measurements. The standard CIO product is derived from radiances measured by the radiometer centered near 640 GHz; CIO is also retrieved using radiances from the 190-GHz radiometer, but these data have poorer precision. The MLS v2.2 CIO data are scientifically useful over the range 100 to 1 hPa. A summary of the precision and resolution (vertical and horizontal) of the v2.2 CIO measurements as a function of altitude is given in Table 2. The impact of various sources of systematic uncertainty has been quantified through a comprehensive set of retrieval simulations. Table 2 also includes estimates of the biases and scaling errors in the measurements compiled from this uncertainty analysis. The systematic uncertainty budget deduced through this set of simulations is, however, inconsistent with a significant artifact apparent in the measurements: a negative bias present in both daytime and nighttime mixing ratios below 22 hPa. Outside of the winter polar vortices, this negative bias can be eliminated by subtracting gridded or zonal mean nighttime values from the individual daytime measurements. In studies for which knowledge of lower stratospheric CIO mixing ratios inside the winter polar vortices to better than a few tenths of a ppbv is needed, however, day – night differences are not recommended and the negative bias must be corrected for by subtracting the value in Table 2 from the measurements at each affected level. The overall uncertainty

for an individual data point is determined by taking the root sum square (RSS) of the precision, bias, and scaling error terms (for averages, the single-profile precision value is divided by the square root of the number of profiles contributing to the average).

[53] Comparisons with a climatology derived from the multiyear UARS MLS data set and correlative data sets from a variety of different platforms have also been presented. A consistent picture emerges that both the amplitude and the altitude of the secondary peak in the ClO profile in the upper stratosphere are well determined by MLS. The latitudinal and seasonal variations in the ClO distribution in the lower stratosphere are also well determined, but the correlative comparisons confirm the existence of a substantial negative bias in the v2.2 MLS ClO data at the lowest retrieval levels.

[54] Quality control should be implemented in any scientific studies using the MLS ClO measurements. Several metrics for evaluating data quality are provided along with the retrieved mixing ratios in the MLS Level 2 files. More detail on these quantities is given in section 2.2. Briefly, any data point for which any of the following conditions are met should be discarded: (1) the associated precision value is negative, (2) "Status" is an odd number, (3) "Quality" is less than 0.8, or (4) "Convergence" is greater than 1.5.

[55] The refinements in the retrieval algorithms between v1.5 and v2.2 led to substantial improvements in most MLS data products. Although cumulatively they resulted in an increase in the severity of the negative bias in ClO at the lowest retrieval levels, nevertheless the v2.2 ClO retrieval is considered more reliable as other compensating errors have been eliminated. We therefore strongly recommend the use of v2.2, rather than v1.5, MLS ClO measurements for scientific studies. Planned changes in version 3 algorithms, including the retrieval of additional species such as CH₃Cl and CH₃OH, should substantially reduce the negative bias present below 22 hPa. Another goal for version 3 is to improve the ClO retrievals at 147 hPa.

[56] Validation of satellite measurements is an ongoing process. It is important to continue to evaluate the quality of the MLS ClO data set, especially in light of future refinements to the data processing software. The analyses presented here can be extended as more v2.2 data become available; at the time of writing (February 2007), fewer than 100 days of MLS data have been reprocessed to v2.2. Recent balloon flights from Kiruna, Sweden during the January/February 2007 campaign, continuing satellite missions, and planned deployments of various instruments during the upcoming International Polar Year, will all afford more opportunities for cross comparisons.

[57] **Acknowledgments.** We are very grateful to the MLS instrument and data operations and development team for their support through all the phases of the MLS project, in particular D. Flower, G. Lau, J. Holden, R. Lay, M. Loo, D. Miller, B. Mills, S. Neely, G. Melgar, A. Hanzel, M. Echeverri, E. Greene, A. Mousessian, C. Vuu, and X. Sabouchi. We greatly appreciate the efforts of Bojan Bojkov and the Aura Validation Data Center (AVDC) team, whose work facilitated the MLS validation activities. Thanks to the Aura Project for their support throughout the years (before and after Aura launch), in particular M. Schoeberl, A. Douglass (also as cochair of the Aura validation working group), E. Hilsenrath, and J. Joiner. We also acknowledge the support from NASA Headquarters: P. DeCola for MLS and Aura and M. Kurylo, especially in relation to the Aura validation activities and campaign planning efforts. The aircraft campaigns themselves involved tireless hours from various coordinators, including E. Jensen and

M. Schoeberl, as well as K. Thompson, and others involved with campaign flight management and support. We express our thanks to the Columbia Scientific Balloon Facility (CSBF) for providing operations services for the balloon experiments whose data are used in this work. Thanks to I. Mackenzie for helpful comments. The anonymous reviewers are thanked for their thoughtful comments. Odin is a Swedish-led satellite project funded jointly by the Swedish National Space Board (SNSB), the Canadian Space Agency (CSA), the National Technology Agency of Finland (Tekes) and the Centre National d'Études Spatiales (CNES) in France. Work at the Jet Propulsion Laboratory, California Institute of Technology, was done under contract with NASA.

References

- Avallone, L. M., and D. W. Toohey (2001), Tests of halogen photochemistry using in situ measurements of ClO and BrO in the lower polar stratosphere, *J. Geophys. Res.*, *106*, 10,411–10,421.
- Barret, B., et al. (2006), Intercomparisons of trace gas profiles from the Odin/SMR and Aura/MLS limb sounders, *J. Geophys. Res.*, *111*, D21302, doi:10.1029/2006JD007305.
- Berthet, G., et al. (2005), Nighttime chlorine monoxide observations by the Odin satellite and implications for the ClO/Cl₂O₂ equilibrium, *Geophys. Res. Lett.*, *32*, L11812, doi:10.1029/2005GL022649.
- Bloom, S. C., et al. (2005), The Goddard Earth Observing Data Assimilation System, GEOS DAS Version 4.0.3: Documentation and validation, *NASA Tech. Rep. 104606 V26*.
- Butchart, N., and E. E. Remsburg (1986), The area of the stratospheric polar vortex as a diagnostic for tracer transport on an isentropic surface, *J. Atmos. Sci.*, *43*, 1319–1339.
- Connor, B. J., T. Mooney, J. Barrett, P. Solomon, A. Parrish, and M. Santee (2007), Comparison of ClO measurements from the Aura Microwave Limb Sounder to ground-based microwave measurements at Scott Base, Antarctica, in spring 2005, *J. Geophys. Res.*, *112*, D24S42, doi:10.1029/2007JD008792.
- Dufour, G., et al. (2006), Partitioning between the inorganic chlorine reservoirs HCl and ClONO₂ during the Arctic winter 2005 from the ACE-FTS, *Atmos. Chem. Phys.*, *6*, 2355–2366.
- Glatthor, N., et al. (2004), Spaceborne ClO observations by the Michelson Interferometer for Passive Atmospheric Sounding (MIPAS) before and during the Antarctic major warming in September/October 2002, *J. Geophys. Res.*, *109*, D11307, doi:10.1029/2003JD004440.
- Kleinböhl, A., et al. (2002), Vortexwide denitrification of the Arctic polar stratosphere in winter 1999/2000 determined by remote observations, *J. Geophys. Res.*, *107*, 8305, doi:10.1029/2001JD001042 [printed 108(D5), 2003].
- Kleinböhl, A., et al. (2005), Denitrification in the Arctic mid-winter 2004/2005 observed by airborne submillimeter radiometry, *Geophys. Res. Lett.*, *32*, L19811, doi:10.1029/2005GL023408.
- Livesey, N. J., et al. (2005), Version 1.5 Level 2 data quality and description document, *Tech. Rep. JPL D-32381*, Jet Propul. Lab., Pasadena, Calif. (Available at <http://mils.jpl.nasa.gov>)
- Livesey, N. J., W. V. Snyder, W. G. Read, and P. A. Wagner (2006), Retrieval algorithms for the EOS Microwave Limb Sounder (MLS), *IEEE Trans. Geosci. Remote Sens.*, *44*, 1144–1155.
- Livesey, N. J., et al. (2007), Version 2.2 Level 2 data quality and description document, *Tech. Rep. JPL D-32381*, Jet Propul. Lab., Pasadena, Calif. (Available at <http://mils.jpl.nasa.gov>)
- Murtagh, D., et al. (2002), An overview of the Odin atmospheric mission, *Can. J. Phys.*, *80*, 309–319.
- Nassar, R., et al. (2006), A global inventory of stratospheric chlorine in 2004, *J. Geophys. Res.*, *111*, D22312, doi:10.1029/2006JD007073.
- Read, W. G., Z. Shippony, M. J. Schwartz, N. J. Livesey, and W. V. Snyder (2006), The clear-sky unpolarized forward model for the EOS Aura Microwave Limb Sounder (MLS), *IEEE Trans. Geosci. Remote Sens.*, *44*, 1367–1379.
- Read, W. G., et al. (2007), Aura Microwave Limb Sounder upper tropospheric and lower stratospheric H₂O and relative humidity with respect to ice validation, *J. Geophys. Res.*, *112*, D24S35, doi:10.1029/2007JD008752.
- Rodgers, C. D. (2000), *Inverse Methods for Atmospheric Sounding: Theory and Practice*, World Sci., Singapore.
- Santee, M. L., G. L. Manney, J. W. Waters, and N. J. Livesey (2003), Variations and climatology of ClO in the polar lower stratosphere from UARS Microwave Limb Sounder measurements, *J. Geophys. Res.*, *108*(D15), 4454, doi:10.1029/2002JD003335.
- Santee, M. L., et al. (2005), Polar processing and development of the 2004 Antarctic ozone hole: First results from MLS on Aura, *Geophys. Res. Lett.*, *32*, L12817, doi:10.1029/2005GL022582.
- Schoeberl, M. R., et al. (2006a), Chemical observations of a polar vortex intrusion, *J. Geophys. Res.*, *111*, D20306, doi:10.1029/2006JD007134.

- Schoeberl, M. R., et al. (2006b), Overview of the EOS Aura mission, *IEEE Trans. Geosci. Remote Sens.*, *44*, 1066–1074.
- Solomon, P., J. Barrett, B. Connor, S. Zoonematkermani, A. Parrish, A. Lee, J. Pyle, and M. Chipperfield (2000), Seasonal observations of chlorine monoxide in the stratosphere over Antarctica during the 1996–1998 ozone holes and comparison with the SLIMCAT three-dimensional model, *J. Geophys. Res.*, *105*, 28,979–29,001.
- Solomon, P., B. Connor, J. Barrett, T. Mooney, A. Lee, and A. Parrish (2002), Measurements of stratospheric ClO over Antarctica in 1996–2000 and implications for ClO dimer chemistry, *Geophys. Res. Lett.*, *29*(15), 1708, doi:10.1029/2002GL015232.
- Solomon, P., J. Barrett, T. Mooney, B. Connor, A. Parrish, and D. E. Siskind (2006), Rise and decline of active chlorine in the stratosphere, *Geophys. Res. Lett.*, *33*, L18807, doi:10.1029/2006GL027029.
- Solomon, S. (1999), Stratospheric ozone depletion: A review of concepts and history, *Rev. Geophys.*, *37*, 275–316.
- Stachnik, R. A., R. Salawitch, A. Engel, and U. Schmidt (1999), Measurements of chlorine partitioning in the winter Arctic stratosphere, *Geophys. Res. Lett.*, *26*, 3093–3096.
- Swinbank, R., N. B. Ingleby, P. M. Boorman, and R. J. Renshaw (2002), A 3D variational data assimilation system for the stratosphere and troposphere, *Tech. Rep. 71*, Met Off., Exeter, UK.
- Toon, G. C., et al. (1999), Comparison of MkIV balloon and ER-2 aircraft measurements of atmospheric trace gases, *J. Geophys. Res.*, *104*, 26,779–26,790.
- Urban, J., et al. (2005), Odin/SMR limb observations of stratospheric trace gases: Level 2 processing of ClO, N₂O, HNO₃, and O₃, *J. Geophys. Res.*, *110*, D14307, doi:10.1029/2004JD005741.
- Urban, J., et al. (2006), Odin/SMR limb observations of trace gases in the polar lower stratosphere during 2004–2005, in *Proceedings of the ESA First Atmospheric Science Conference, 8–12 May 2006, Frascati, Italy*, edited by H. Lacoste, *Eur. Space Agency Spec. Publ., ESA-SP-628*.
- von Clarmann, T., et al. (2005), Experimental evidence of perturbed odd hydrogen and chlorine chemistry after the October 2003 solar proton events, *J. Geophys. Res.*, *110*, A09S45, doi:10.1029/2005JA011053.
- von Hobe, M., J.-U. Groöb, R. Müller, S. Hrechanyy, U. Winkler, and F. Stroh (2005), A re-evaluation of the ClO/Cl₂O₂ equilibrium constant based on stratospheric in-situ observations, *Atmos. Chem. Phys.*, *5*, 693–702.
- von Hobe, M., et al. (2006), Severe ozone depletion in the cold Arctic winter 2004–05, *Geophys. Res. Lett.*, *33*, L17815, doi:10.1029/2006GL026945.
- Waters, J. W. (1993), Microwave limb sounding, in *Atmospheric Remote Sensing by Microwave Radiometry*, edited by M. A. Janssen, chap. 8, pp. 383–496, John Wiley, New York.
- Waters, J. W., L. Froidevaux, W. G. Read, G. L. Manney, L. S. Elson, D. A. Flower, R. F. Jarnot, and R. S. Harwood (1993), Stratospheric ClO and ozone from the Microwave Limb Sounder on the Upper Atmosphere Research Satellite, *Nature*, *362*, 597–602.
- Waters, J. W., et al. (2006), The Earth Observing System Microwave Limb Sounder (EOS MLS) on the Aura satellite, *IEEE Trans. Geosci. Remote Sens.*, *44*, 1075–1092.
- World Meteorological Organization (2007), Scientific assessment of ozone depletion: 2006, *Global Ozone Res. and Monit. Proj. Rep. 50*, Geneva, Switzerland.
-
- B. Barret and P. Ricaud, Laboratoire d'Aérodynamique, CNRS, 14 Avenue Edouard Belin, Toulouse, F-31400 France.
- R. E. Cofield, D. T. Cuddy, W. H. Daffer, B. J. Drouin, L. Froidevaux, R. A. Fuller, R. F. Jarnot, A. Kleinböhl, B. W. Knosp, A. Lambert, N. J. Livesey, V. S. Perun, W. G. Read, M. L. Santee (corresponding author), W. V. Snyder, R. A. Stachnik, P. C. Stek, R. P. Thurstans, G. C. Toon, P. A. Wagner, and J. W. Waters, Jet Propulsion Laboratory, 4800 Oak Grove Drive, Pasadena, CA 91109, USA. (mls@mls.jpl.nasa.gov)
- B. Connor, National Institute of Water and Atmospheric Research, Lauder, Private Bag 50061, Omakau, Central Otago, New Zealand.
- H. Küllmann, Institute of Environmental Physics, University of Bremen, Bremen, Germany.
- J. Kuttippurath, LMD/CNRS Ecole Polytechnique, F-91128 Palaiseau, France.
- G. L. Manney, Department of Physics, New Mexico Institute of Mining and Technology, Socorro, NM 87801, USA.
- D. Murtagh and J. Urban, Department of Radio and Space Science, Chalmers University of Technology, SE-41296 Göteborg, Sweden.
- M. von Hobe, Institut für Chemie und Dynamik der Geosphäre I: Stratosphäre, Forschungszentrum Jülich, D-52425 Jülich, Germany.